공학석사 학위논문

해상 유출유의 화학적 분산 능력 분석 및 공간적인 두께 분포를 고려한 회수 능력 산정 모델 개발

Analysis of Chemical Dispersion Potential of Oil Spilled at Sea and Development of a Model to Estimate Recovery Potential Considering Spatial Thickness Distribution

지도교수 허 철

2019년 2월

한국해양대학교 해양과학기술전문대학원

해양과학기술융합학과
최 윤 선

본 논문을 최윤선의 공학석사 학위논문으로 인준함.

위원장	도 기 덕	(인)
위 원	허 철	(인)
위 원	박 영 규	(인)

2018년 12월 27일

한국해양대학교 해양과학기술전문대학원

Contents

List of Tables

List of Figures

해상 유출유의 화학적 분산 능력 분석 및 공간적인 두께 분포를 고려한 회수 능력 산정 모델 개발

최윤선

해양과학기술융합학과
해양과학기술전문대학원

Abstract

유처리제를 사용하여 기름이 화학적으로 분산되는 양은 해상 조건이나 유류의 특성에 따라 달라진다. 본 연구에서는 풍화작용에 따른 유류 특성 변화, 그에 따른 기름의 화학적 분산량을 추산하는 알고리즘을 개발하였다. 또한 유처리제 사용량과 화학적 분산량과의 상관관계를 정량적으로 분석하기 위해 유처리제 살포량, 분산 효율 및 살포 기간에 대한 민감도 분석을 수행하였다. 개발된 모델을 허베이 스피리트호 유류 오염 사고에 적용하여 화학적 분산량을 추정하기 위한 비교 계산을 수행하였다. 계산 결과, 15일 동안 300 *kl*의 유처리제를 나누어 사용한 경우 화학적 분산량은 625 *kl*로 나타났다. 또한, 민감도 분석 결과를 바탕으로 동일한 방제 제원 조건에서 최소한의 유처리제 양으로 동일한 분산량을 얻기 위해 계산한 결과, 5시간 동안 105 *kl*의 유처리제 사용이 필요한 것으로 나타났다. 이는 유처리제 살포 기간이 14일 줄어들고 살포량이 1/3로 감소함을 의미한다. 따라서 본 연구를

통해 도출된 모델을 이용하여 동일한 화학적 분산 효과를 얻기 위한 유처리제 살포 기간 및 살포량을 최소화할 수 있을 것이다.

해상에서의 유출유에 대한 회수 모델링 및 대응 연구는 많이 진행되어왔다. 그러나 풍화작용, 기름 특성, 장비 효율을 모두 고려하여 회수 능력을 산정하는 연구는 여전히 부족하다. 본 연구에서는 회수 능력을 산정하기 위한 두 가지 모델을 개발했다. 하나는 이러한 특성을 반영하여 회수 능력을 산정하는 공간적으로 균일한 모델이다. 다른 하나는 이러한 특성뿐만 아니라 회수에 의한 공간적인 두께 변화도 고려하는 공간적으로 불균일한 모델이다. 사고 시나리오를 사용한 계산을 통해 두 모델간의 비교를 수행하였으며 이것이 방제에 미치는 영향을 분석하였다. 계산 결과, 공간적으로 불균일한 모델에서는 공간적으로 균일한 모델에서 확인할 수 없었던 얇은 유막, 자연적인 소산을 확인하였으며 배치 가능한 회수 시스템의 정량화를 분석하는 것이 가능했다. 최종적으로 유출유의 해상 잔존량과 회수 시스템의 방제 시간 및 수량과의 상관관계를 분석하였다.

KEY WORDS: Oil spill 기름 유출; Response 방제; Weathering 풍화작용; Chemical dispersion potential 화학적 분산 능력; Recovery potential 회수 능력.

Chapter 1 Introduction

1.1 Introduction to spilled oil response at sea

Oil consumption has been increased around the world (World Energy Conusil (WEC), 2016; British Petroleum, 2017). Although oil spill accidents at sea have decreased, large and small accidents still occur (Musk, 2011). Thus, as long as oil transport and consumption are maintained or increased, we must continue to be prepared for and respond to oil spill accidents. The techniques to be employed at sea include containment and recovery, chemical dispersants, and controlled(in-situ) burning (International Petroleum Industry Environmental Conservation Association (IPIECA) & International Association of Oil and Gas Producers (IOGP), 2015). Mechanical recovery is a method to remove spilled oil while minimizing environmental impact (IPIECA & IOGP, 2015). Oil treatment agents promote oil dispersion by reducing the interfacial tension between oil and water. Underwater distributed oil is less wind-imposed, which can reduce the degree of access to coast or sensitive area (International Tanker Owners Pollution Federation Limited (ITOPF), 2014). In-situ buring can quickly remove a lot of oil. (IPIECA & IOGP, 2015). In Korea, oil recovery through oil skimmer is the main method used for oil spill in sea. The dispersant is applied in some situations and burning is not considered (Kim, et al., 2016). The response technology for the skimmer and the dispersant are dealt with in this paper.

Research pertaining to effective response planning for oil spills at sea can be classified broadly into remote sensing, trajectory modeling, spill modeling, and countermeasures (Fingas, 2016). This study focuses on recovery at sea through spill modeling and countermeasure planning; these topics can be further divided into oil properties, weathering, and response categories. Numerous studies have been conducted on spilled oil properties (Antoine, 1888; Mooney, 1951; Jokuty, et al., 1995; Song & Springer, 1996; Fingas & Fieldhouse, 2009, 2012) and weathering (Monahan, 1971; Mackay & Matsugu, 1973; Payne, et al., 1984; Delvigne & Sweeney, 1988; Eley, et al., 1988; Zelenke, et al., 2012). Mackay and Matsugu (1973) researched the evaporation rate of spilled oil, and Delvigne and Sweeney (1988) investigated natural dispersion. These studies associated sea state and the properties of the spilled oil with the weathering process, but did not estimate the changes in oil properties caused by weathering.

The properties of spilled oils undergo continuous change with time due to weathering processes such as spreading, evaporation, emulsification, and dispersion (Spaulding, 1988; Sebastião & Guedes Soares, 1995; Reed, et al., 1999). Mackay, et al. (1982) developed an oil spill behavior model that encompasses weathering and changes in oil properties, and Berry, et al. (2012) modeled oil transport and fate processes. However, these studies did not include prediction of the response potential.

The performance of response equipment varies with oil fates and sea conditions and is a critical factor as it has a direct effect on clean-up potential calculations (Lehr, 2001). Strom-Kristiansen, et al. (1993) represented the dispersion efficiency as a function of viscosity through experiments, United States Coast Guard (USCG) (1994) explored the relationship between burning efficiency and oil layer thickness, and Lorenzo, et al. (1995) determined the recovery efficiency based on the rotation speed of skimmer and the oil viscosity. Clean-up potential is affected by oil property, sea state, weathering, performance of response equipment (ITOPF, 2014). Therefore, all of the above studies should be linked to estimate the clean-up potential, but these studies are insufficient.

1.2 Necessity for analysis of the chemical dispersion considering the dispersant dosage and change of oil properties by weathering

Dispersant can be used under conditions where mechanical recovery is difficult. Also, it is recognized as effective control means capable of rapidly processing large areas (Lessard & Demarco, 2000). Approximately 7,950 *kl* of dispersant was used for Deepwater Horizon oil spill (2010) in the Gulf of Mexico (Kujawinski, et al., 2011). In the case of the Hebei Spirit oil spill in Korea (2007), about 300 *kl* of dispersant was used (Korea Maritime Institute (KMI), 2008).

However, the toxicity of crude oil (Almeda, et al., 2013; Rico-Martinez, et al., 2013), dispersant (Almeda, et al., 2014; Wise & Wise, 2011), and chemically dispersed oil (Cohen, et al., 2014; Goodbody-Gringley, et al., 2013) can have a impact on marine life. Therefore, careful decision is needed when using dispersant (Hong, et al., 2014; Lee, et al., 2006). Although the usefulness of dispersant has been proven, most countries apply restrictively dispersant due to the negative effects mentioned above (Cho & Ha, 2012), and the area where the dispersant can be sprayed is designated as water depth and distance from coast (Korea Institute of Ocean Science and Technology (KIOST), 2010). Limited use of dispersant is considered based on water depth, distribution of sensitive areas, and sea flow characteristics in Korea (Lee, et al., 2006). Therefore, in order to mitigate negative concerns, it would be very useful to reduce the application amount of dispersant while obtaining the same dispersion effect. For this purpose, it is necessary to understand the quantitative correlation between the dispersant amount and the amount of chemical dispersion.

The amount of chemical dispersion also varies depending on the timing of the use of dispersant, since the characteristics of the spilled oil are continuously changed by weathering effects in case of oil spill in the sea. Thus, it is necessary to take into account change in the oil characteristics with time due to weathering, when estimating the amount of chemical dispersion. However, researches that can quantitatively analyze the correlation between dispersant amount and the amount of residual oil on the sea and utilize it for the response strategy are very insufficient (Zhong & You, 2011).

The U.S. National Oceanic and Atmospheric Administration (NOAA) developed Automated Data Inquiry for Oil Spills 2 (ADIOS2; Lehr, et al., 2002) that calculates weathering of the spilled oil. This model calculates spreading, evaporation, natural dispersion, and emulsification of oil. In addition, ADIOS2 provide users with options for chemical dispersion, mechanical recovery, in-situ burning, and beaching, thereby estimating the residual oil volume according to the marine spillage removal option selected. However, this removal options adopt a method of estimating by the user rather than calculating the removal amount according to the sea state or the characteristics of the spilled oil. That is, in the case of the chemical dispersion option, the amount of chemical dispersion is calculated through a constant input by the user as how much oil slick is to be treated and how efficient the dispersant is. Therefore, the calculated dispersion amount is derived as a constant value regardless of the time. However, as mentioned above, the amount of chemical dispersion varies continuously with time. As a result, the ADIOS2 model has a limitation in that it does not take into account changes in the oil characteristics with time. Also, through the calculation of ADIOS2, the quantitative correlation between the amount of dispersant and the amount of chemical dispersion can not be known.

The purpose of this study is to quantitatively analyze the correlation between dispersant dosage and amount of marine residual oil. A numerical study was conducted to estimate the chemical dispersion amount according to the dispersant dosage and spraying period, at the same time considering the weathering effects. The correlation between the amount of the dispersant and the residual oil derived from this study could be utilized in establishing the response strategy using the dispersant in case of oil spill at sea.

1.3 Necessity for analysis of the mechanical recovery considering the spatial thickness distribution

Estimated Recovery System Potential (ERSP; Allen, et al., 2012; Bureau of Safety and Environmental Enforcement (BSEE) & Genwest System, Inc., 2015) is a planning tool that estimates the recovery potential based on the oil thickness; ERSP considers skim, transit and offloading/rigging time related to the skimming capacity, efficiency, and on-board tankage in the recovery calculation. However, this model doesn't reflect oil properties and environmental conditions. Furthermore, it has a limitation, though the model includes the tendency of spreading and emulsification among weathering factors and the efficiency of recovery equipment. It is because these factors are represented as relatively simple constants.

Response Options Calculator (ROC; Galt & Overstreet, 2009; Dale, 2011) is a response model used to calculate aspects of the clean-up potential, such as recovery, chemical dispersion, and in-situ burning, by reflecting weathering and changes in spilled oil properties and equipment efficiency. ROC also calculates recovery rates based on oil thickness and includes the time spent on skimming, transit, and offloading/rigging activities as in ERSP. ROC considers the substantial role played by weathering in thickness variation, and the recovery efficiency is calculated over time and applied. The oil characteristics, such as density, viscosity, and distillation cut, and environmental conditions, such as water temperature and wind speed, are included in these calculations.

Lots of studies related to recovery potential consider weathering, changes in oil properties, and equipment efficiency were carried out. But the models and studies to compare and analyze the effect of the oil thickness distribution by oil recovery are insufficient. It is not easy to quantitatively grasp the effect of the oil thickness distribution of the skimmed space on recovery amount using the existing study. Therefore, two models were developed in this study. One is a spatially uniform model and the other is a spatially nonuniform model considering the spatial thickness variation by skimming. Recovery potential and its effect on response were compared and analyzed using two models.

1.4 Organization of thesis

This thesis was written based on registered papers and research contents.

In Chapter 2, a model was developed to estimate chemical dispersion potential and the correlation between dispersant dosage and chemically dispersed oil volume was quantitatively analyzed. Also this contents cited a study paper (Choe, et al., 2018).

In Chapter 3, a spatially nonuniform model considering the spatial thickness variation by skimming was developed. this model was compared with a spatially uniform model. Also this contents cited a study paper (Choe, et al., under review).

Chapter 2 Analysis of Estimation of chemical dispersion amount considering the dispersant dosage and change of oil properties by weathering

2.1 Methods for estimating chemical dispersion potential

2.1.1 Algorithm for estimating weathering and chemical dispersion of spilled oil

Algorithm for estimating oil properties, weathering, and dispersion potential of dispersant consists of spreading, evaporation, natural dispersion, emulsification, and chemical dispersion. Oil spilled to the sea spreads and the oil properties change continuously due to weathering. Therefore, each of the above elements was calculated at one hour intervals, to reflect this change in characteristics, and result values become input values at the next time step. Flow chart of the model’s calculation algorithm is shown in Fig. 1.

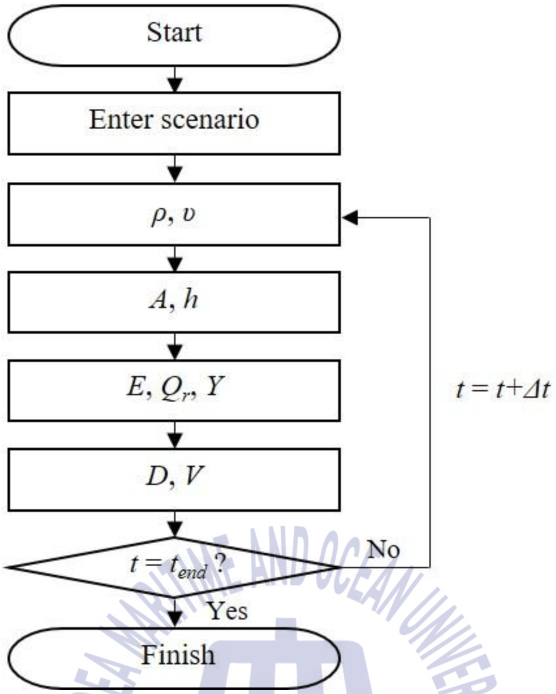

Fig. 1 Flow chart of calculation algorithm (Choe, et al., 2018)

In Fig. 1, V is volume of remaining oil (*kl*), t_{end} is end time of simulation (s), and the remaining symbols are described in the following equations.

The oil begins to spread as soon as it spills into the sea, resulting in a large increase of oil slick area. The spreading equation of Fay (1969) was used to calculate the slick area. The area is expressed as a function of oil amount initially spilled, density (ρ), viscosity (ν), and time (t) and spreads further by wind.

The amount of evaporation was calculated through the mass transfer equation (Mackay & Matsugu, 1973) to estimate the amount of oil evaporation. The evaporation rate is affected by factors such as wind speed, slick area, and water temperature as shown in Eq. (1) and the vapor pressure of each component is used respectively to calculate the evaporation rate by introducing the concept of pseudo component (Payne, et al., 1984):

$$\frac{dE_i}{dt} = \frac{K_i U^{\frac{7}{9}} A \overline{V_i} \chi_i P_i}{RT} \quad (1)$$

where E is evaporation volume (kl), i is number of pseudo component, K is mass transfer coefficient, U is wind speed (m/s), A is area of the spill (m^2), $\overline{V}$ is molar volume (m^3/mole), χ is mole fraction, P is vapor pressure (Pa), R is gas constant (8.314 Pa · m^3/mol · K), T is ambient temperature (K).

Natural dispersion of oil is calculated by using entrainment rate equation (Delvigne & Sweeney, 1988). The equation of entrainment rate is as shown Eq. (2):

$$Q_r = C_0 D_{ba}^{0.57} S_{cov} F_{wc} d_o^{0.7} \quad (2)$$

where Q_r is entrainment rate of oil droplets (kg/m^2s), C_0 is function of oil viscosity and volume fraction of water, D_{ba} is dissipated breaking wave energy per unit surface area (J/m^2), S_{cov} is fraction of sea surface covered by oil. F_{wc} is fraction of sea surface hit by breaking waves per unit time (s^{-1}) and function of wind speed. d_o is oil droplet size (mm). The amount of natural dispersion is determined by multiplying the calculated entrainment rate, area, and time.

Eley's equation (Eley, et al., 1988) which is expressed as Eq. (3) is used to calculate water fraction due to emulsification of spilled oil:

$$\Phi = \frac{S_c d_{sv}}{6 + S_c d_{sv}} \quad (3)$$

where Φ is volume fraction of water. S_c is interfacial area of oil-water (m^2cm^{-3}), and it is function of wind speed, oil density, and viscosity. d_{sv} is surface area per unit volume mean diameter (μm).

The amount of chemical dispersion that can be obtained by using dispersant is calculated through following process. Encounter volume where dispersant is sprayed during the time step (Δt) is found using Eq. (4) (American Society for Testing and Materials (ASTM), 2013; ASTM, 2015):

$$EV = h * w * v * \Delta t \tag{4}$$

where *EV* is encounter volume (㎘), *h* is slick thickness (m), *w* is swath width (m), *v* is application speed (m/s), Δt is time step (3600 s).

Finally, the volume of chemical dispersion is calculated using Eq. (5) (ASTM, 2013; ASTM, 2015; Fingas, 2010):

$$D = \frac{d}{DOR} * DE \tag{5}$$

where *D* is volume of chemical dispersion (㎘), *d* is dosage volume (㎘), *DOR* is dispersant to oil ratio, *DE* is dispersant efficiency. As a result of calculation of Eq. (5), if *d/DOR* is greater than *EV*, *d/DOR* is replaced with *EV* to calculate chemical dispersion.

2.1.2 Dispersion efficiency of dispersant

Dispersant efficiency which is expressed in Eq. (5) is defined as the amount of oil that the dispersant puts into the water column compared to the amount of oil that remains on the surface (Fingas, 2010). The results of the preceding study on the dispersant efficiency are as follows. First, ECO-CLEAN (Daemyung Chemical Co., Ltd.), one of the dispersant used in Korea, showed little effect when the kinematic viscosity of oil is more than 2,000 cSt and is not effective when the oil viscosity is more than 5,000 cSt. Efficiencies were 91.1% at 30 seconds and 41.5% at 10 minutes (Daemyung Chemical, 2005). Jin, et al. (2015) experimented with 3 types of crude oil and 4 items of domestic dispersant and the results were expressed as dispersant efficiencies after 30 seconds and 10 minutes. In addition, KIOST (2009) measured dispersant efficiency from 20 minutes to 48 hours for one foreign dispersant and one domestic dispersant. However, in this study, it is difficult to directly utilize the previous research data mentioned above since the dispersant efficiency is required for wind speed and viscosity. Therefore, the efficiency data of the dispersant from abroad was used. If related data on domestic dispersant are secured in the future, it will be possible to conduct research using them.

Allen & Dale (1995) showed the dispersant efficiencies as function of wind speed and viscosity. Reconstructed data to utilize these efficiencies to calculation algorithm in this study are shown in Figs. 2 and 3. Fig. 2 shows the dispersion efficiency of the dispersant according to the wind speed. Fig. 3 shows the dispersion efficiency of the dispersant according to the viscosity. Performance test of the dispersants were carried out by MNS (Mackay & Szeto, 1980) test and IFP (Institute Francais du Petrole; Bocard, et al., 1984) test using Corexit 9527(United States Environmental Protection Agency (EPA), 2018) and are presented in the range represented by maximum and minimum values respectively.

MNS test was estimated to correspond to medium to high wave energy by using wind-induced energy. IFP test is that energy is transmitted in the water column by a ring that moves up and down and corresponds to relatively low wave energy (Brandvik, et al., 2010; Renard, et al., 1995). In this study, the dispersant efficiency of Allen and Dale was applied to the model. In the calculation, the dispersant efficiency was taken by obtaining the dispersion efficiency of the dispersant according to the wind speed and the viscosity and using a lower value. Small amount of dispersion is estimated by using lower efficiency, thereby preventing the dispersion effect from being overestimated.

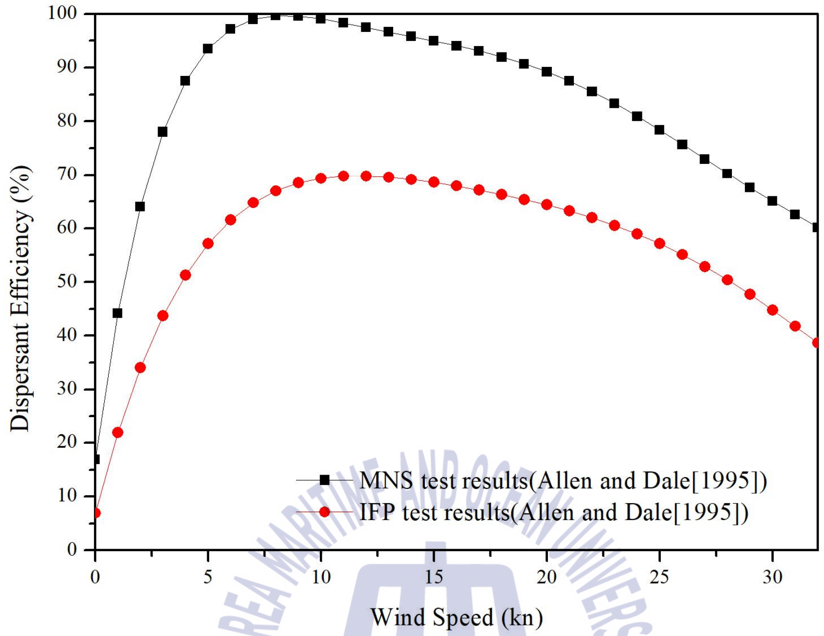

Fig. 2 Dispersant application performance with wind speed (Choe, et al., 2018)

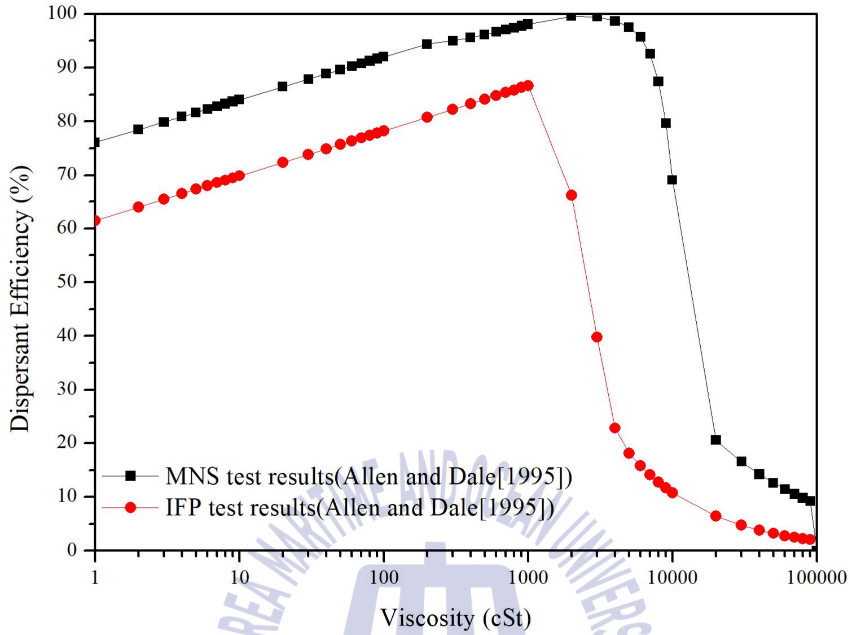

Fig. 3 Dispersant application performance with viscosity (Choe, et al., 2018)

2.2 Sensitivity analysis of chemical dispersion amount according to spraying the dispersant

Three sensitivity analyses were performed to evaluate the chemical dispersion of developed modeling. Three parameters for the sensitivity analysis are dispersant dosage, efficiency, and spraying period. First, the case of spraying the dispersant in a constant amount and the case of spraying the dispersant amount required to disperse all the oil slick encountered by response were compared. Next, the dispersion amount was calculated using two dispersant efficiency data based on the viscosity since the dispersion amount of oil varies depending on the dispersant efficiency. Finally, cases of spraying the same amount of dispersant for three days and one day respectively were compared.

2.2.1 Setting up a virtual accident scenario

A virtual scenario was set as follows in order to grasp amount of chemical dispersion through the sensitivity analyses. 1000 *kl* of Arabian Heavy is spilled on sea of Busan with wind speed of 3 m/s and water temperature of 14 ℃ at 5 a.m. It is assumed that only oil treatment agent is used for the response. Response vessel No. 18 with dispersant tank of 37 *kl* is mobilized. It starts spraying from the sunrise time at 7 a.m. two hours after the accident, and it is finished spraying at 5 a.m. because of sunset. Dispersant is used same time next day, and a total of 30 *kl* dispersant is used for 3 days and 10 hours a day. Simulation time is 72 hours in total. The oil treatment agent was assumed to use Corexit 9527. Dispersion efficiencies of Figs. 2 and 3 are applied. This is basic case. Table 1 shows the setting values for chemical dispersion amount. The values in Table 1 apply equally to all sensitivity studies.

Table 1 Calculation conditions for a hypothetical scenario (Choe, et al., 2018)

Oil	Arabian Heavy
° API	27.4
Viscosity	48 cSt @16 ℃
Spilled Volume	1,000 *kl*
Wind Speed	3 m/s
Water Temperature	14 ℃
Simulation Time	72 h
Swath Width	10 m
Application Speed	5 kn
DOR	0.05

2.2.2 Estimation of the amount of chemical dispersion according to dosage rate of dispersant

In the first sensitivity study, the case of spraying the dispersant in a constant amount and the case of spraying the dispersant amount required to disperse all the oil slick encountered are compared. The basic case is applied by uniformly spraying 1 *kl* of dispersant per hour. The comparative case has a condition applying the amount of the dispersant required to disperse all of the amount of encounter volume obtained through Eq. (4). Because the oil thickness, h, changes due to spreading of oil in calculation process of Eq. (4), encounter volume varies with time. The amount of the dispersant for dispersing all the encounter volume of the comparative case was obtained by using the chemical dispersion amount, D, of Eq. (5) and the encounter volume, EV, of Eq. (4). Table 2 summarizes the dispersant amount applied per hour for the basic case and the comparative case. Likewise, dispersing all of the encounter oil is the fastest way to remove remaining oil in this sensitivity analysis. If the required dosage rate is greater than the maximum spray rate of the dispersant of response vessel No. 18, the dosage rate of the dispersant is adjusted to the maximum spray rate. The comparative case was assumed to be capable of providing all of the required amount of dispersant in addition to the dispersant storage tank of response vessel No. 18.

Table 2 Comparison of calculation conditions of sensitivity analysis of dispersant dosage (Choe, et al., 2018)

Case	Basic case	Comparative case
Dosage rate	1 *kl*/h	DOR * EV / DE

At the beginning of oil spill, slick thickness is relatively thick compared to elapsed time. Therefore, according to Eq. (4), it is possible to obtain more encounter volume at the beginning of spill and disperse more oil. Fig. 4 shows dosage rate and the remaining oil amount in the basic case ('Fixed') in which the dosage rate is set to 1 *kl* per hour, and in the comparative case ('Required') in which it is assumed that all of encounter volume are dispersed. And 'No dosage' case where there are only evaporation and natural dispersion without spraying the dispersant is shown in Fig. 4. (a) and (b) in Fig. 4 were calculated by applying high dispersion efficiency (MNS test) and low dispersion efficiency (IFP test) respectively. As can be seen in the Fig. 4, the comparative case, which is able to disperse the maximum encounter volume, has less remaining oil than the basic case after 72 hours. The final dispersant dosage volume, chemical dispersion volume, and remaining oil volume after 3 days are shown in Table 3. The difference in the chemical dispersion volume between the high efficiency and the low efficiency is compared with 289 *kl* and 385 *kl* higher than the basic case, respectively. Especially, the volume of chemical dispersion was more than two times at high efficiency, though the volume of dispersant dosage in the basic case and the comparative case were similar. There are differences of 142~237 *kl* of the remaining oil volume between the 'no dosage' case and the basic case. In addition, there is a result that difference between the remaining oil volume in the 'no dosage' case and 253 *kl* in high efficiency of the comparative case is 467 *kl*.

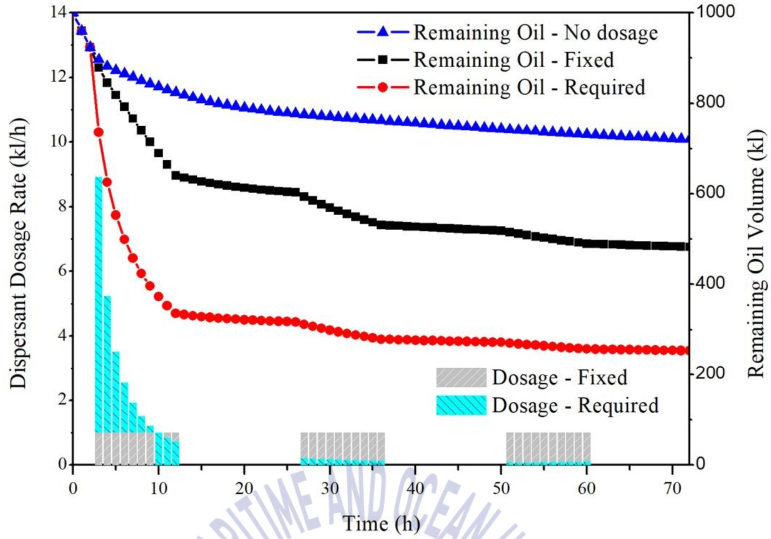

(a) High

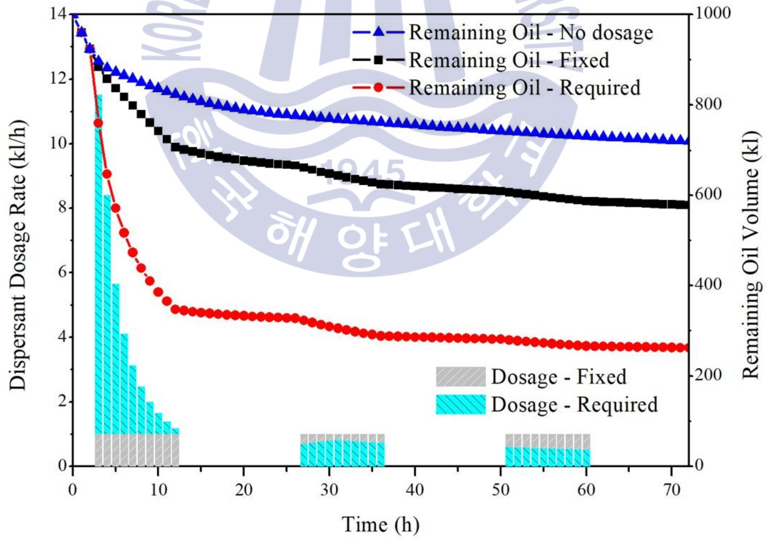

(b) Low

Fig. 4 The dispersant dosage rate and remaining oil volume over time for no dosage case, basic case('Fixed') and comparative case(' Required'); (a) High dispersant efficiency, (b) Low dispersant efficiency (Choe, et al., 2018)

Table 3 Chemically dispersed oil volume and residual oil volume of sensitivity study on dispersant dosage during 3 days (Choe, et al., 2018)

Case	No Dosage	Fixed (Basic)		Required (Comparative)	
		High	Low	High	Low
Dispersant Dosage (*kl*)	-	30	30	29.9	54.5
Chemical Dispersion (*kl*)	-	272	164	561	549
Remaining Oil (*kl*)	720	483	578	253	262

Total amount of 41 *kl* is required in low dispersion efficiency of the comparative case. Therefore, if the dispersant storage tank of 37 *kl* is mobilized alone, there will be a situation where dispersant is not enough. For this reason, another vessel capable of supplying 4 *kl* of dispersant in addition to the response vessel No.18 is required. It is possible to estimate the optimum amount of dispersant over time after the accident through this calculation result. It will help establish response strategies.

2.2.3 Estimation of the amount of chemical dispersion according to dispersion efficiency of dispersant

The second sensitivity analysis is when the dispersion efficiency of the dispersant is changed. Strøm-Kristiansen, et al. (1993) conducted experiments to estimate the correlation between the oil viscosity and the performance of dispersant. The dispersant efficiency was obtained through MNS and IFP tests using Alaskan North Slope (ANS) and Corexit 9527. The reconstructed data for use in this study is illustrated in Fig. 5.

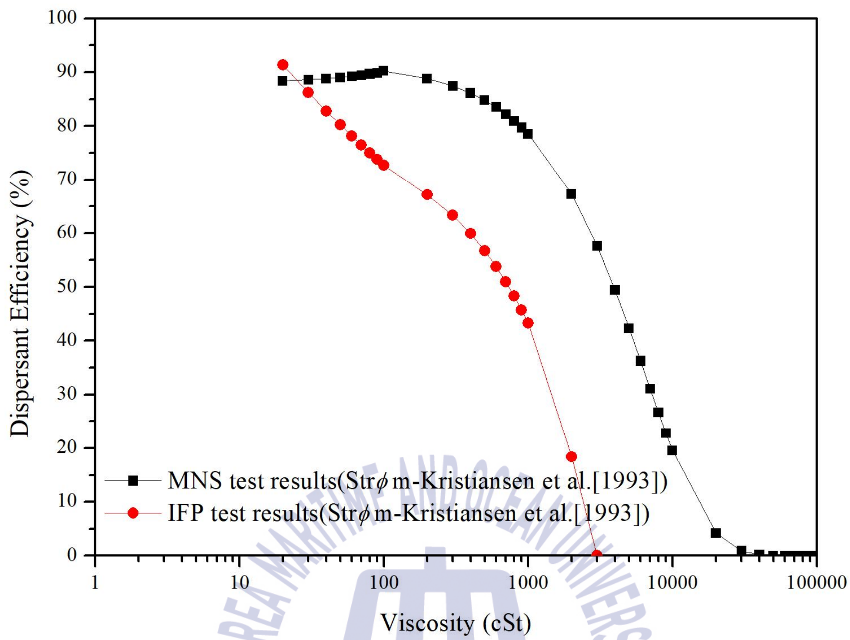

Fig. 5 Effectiveness of the dispersing agents Corexit 9527® according to viscosity (Choe, et al., 2018)

As shown in Eq. (5), the amount of chemical dispersion also varies as the dispersion efficiency, *DE*. The dispersant efficiency of Figs. 2 and 3 were applied to the basic case and the dispersant efficiency of Figs. 2 and 5 were applied to the comparative case. In each case, the dispersion efficiency according to the wind speed and the dispersion efficiency according to the viscosity were calculated. The lower efficiency value of two was applied and the calculation was performed for the MNS test efficiency ('High efficiency') and the IFP test efficiency ('Low efficiency') respectively.

Fig. 6 shows the dispersion efficiency over time. The oil become more viscous due to evaporation and emulsification. This tends to reduce both the dispersion efficiencies used in the basic case and the comparative case. Thus, the chemical dispersion rate is reduced if the dispersant is used at a point when viscosity has increased over a period of time after the accident.

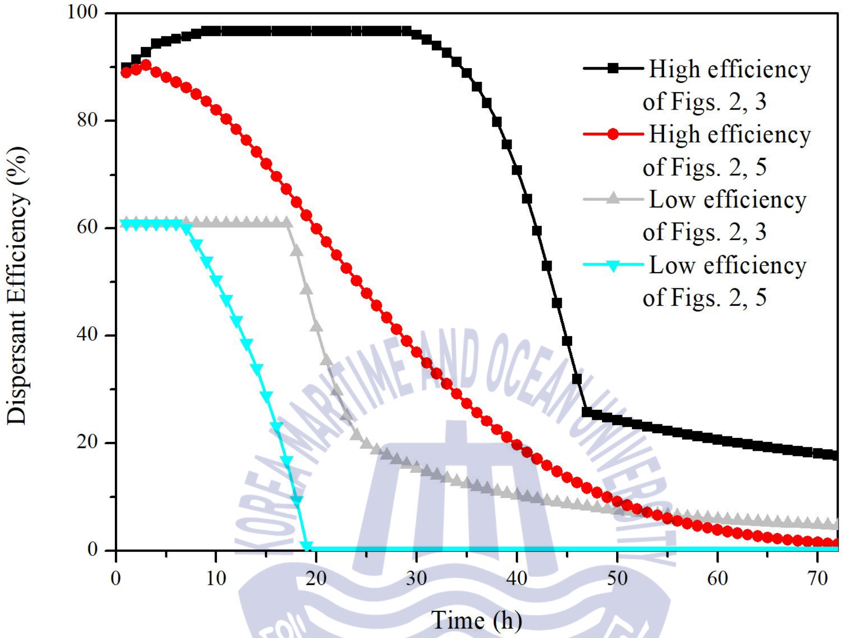

Fig. 6 Dispersion efficiency variation over time (Choe, et al., 2018)

Chemical dispersion rate rapidly decreases than initial one as Fig. 7, because, the dispersion efficiency decreases over time as Fig. 6. also. It can be seen that over time, the decrease is rapid compared to the initial one, as shown in 7. In the low efficiency of Fig. 5, the oil at approximately 3000 cSt indicates no dispersion of dispersant. The result of the simulation shows that the viscosity will be more than 3000 cSt after 20 hours. This is why calculation using the low efficiency of Fig. 5 doesn't have the dispersion rate after 20 hours. Therefore, the chemical dispersion cannot be shown at from second day in Fig. 7. Based on the above results, spraying dispersant is recommended at the beginning of an accident. Table 4 shows the volume of chemical dispersion and remaining oil during 3 days.

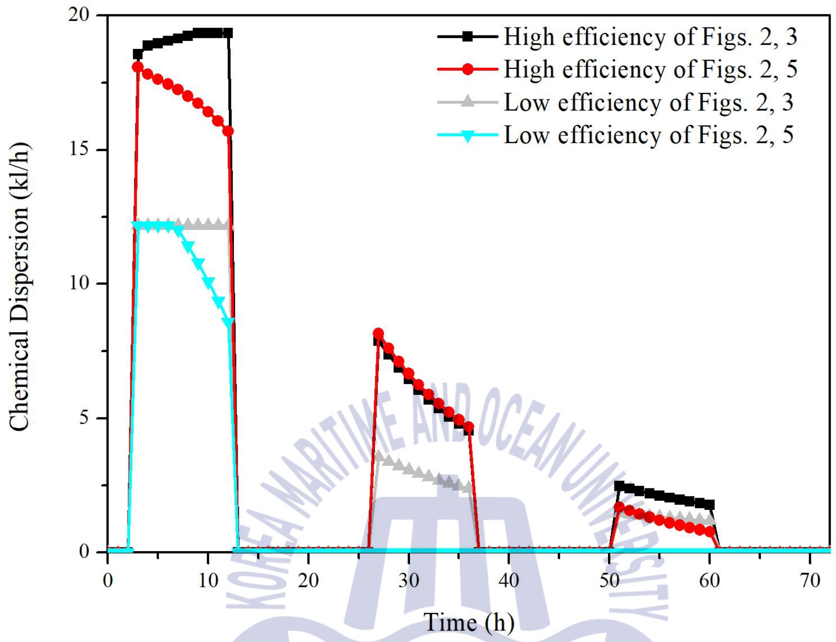

Fig. 7 Chemical dispersion rate according to dispersion efficiency of dispersant (Choe, et al., 2018)

Table 4 Chemically dispersed oil volume and residual oil volume of sensitivity study on dispersant efficiency during 3 days (Choe, et al., 2018)

Case	No Dosage	Efficiency of Figs. 2 & 3 (Basic)		Efficiency of Figs. 2 & 5 (Comparative)	
		High	Low	High	Low
Chemical Dispersion (㎘)	-	272	164	244	111
Remaining Oil (㎘)	720	483	578	508	628

2.2.4 Estimation of the amount of chemical dispersion according to dosage period of dispersant

The amount of chemical dispersion varies depending on the amount and period of spraying the dispersant. The basic case ('Long') using 30 *kl* of dispersant for 3 days is compared with the comparative case ('Short') using same amount for a day in third sensitivity study (Fig. 8).

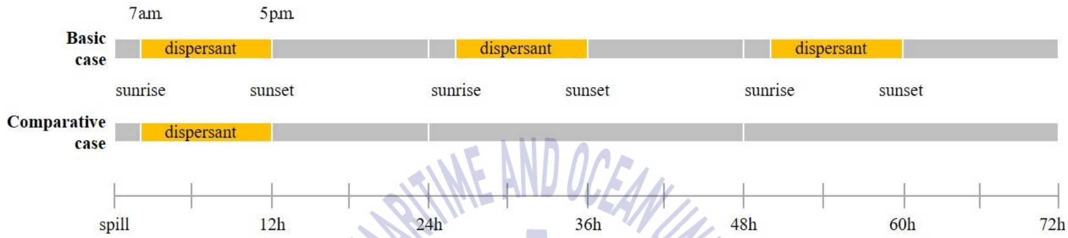

Fig. 8 Comparison of calculation conditions for sensitivity analysis of dosage period of dispersant (Choe, et al., 2018)

According to the result using dispersion efficiency of FIgs. 2 and 3 as can be seen in Fig. 6, the efficiency starts to decrease at about 30 hours in high efficiency and at about 18 hours in low efficiency. Thus, the chemical dispersion effects will be maximized when dispersant can be used intensively within this time. That is to say, the optimal period for spraying the dispersant can be derived.

Fig. 9 shows the amount of chemical dispersion and remaining oil by dosage period for high efficiency case. Despite the same amount of total dispersant, it can be seen that intensive spraying of large amounts during a day can lead to more chemical dispersion than to steadily spray smaller amount over 3 days. Fig. 10 shows the calculation results of the residual oil volume according to the spraying period. As above confirmed, the comparative case has more chemical dispersion volume and less the remaining oil volume than the basic case. Those are compared in Table 5. In the comparative case, the volume of chemical dispersion was found to be 329~406 *kl* by using the dispersant of 30 *kl*.

Table 5 Chemically dispersed oil volume and residual oil volume of sensitivity study on dispersant dosage period during 3 days (Choe, et al., 2018)

Case	No Dosage	Long (Basic)		Short (Comparative)	
		High	Low	High	Low
Chemical Dispersion (*kl*)	-	272	164	406	329
Remaining Oil (*kl*)	720	483	578	382	444

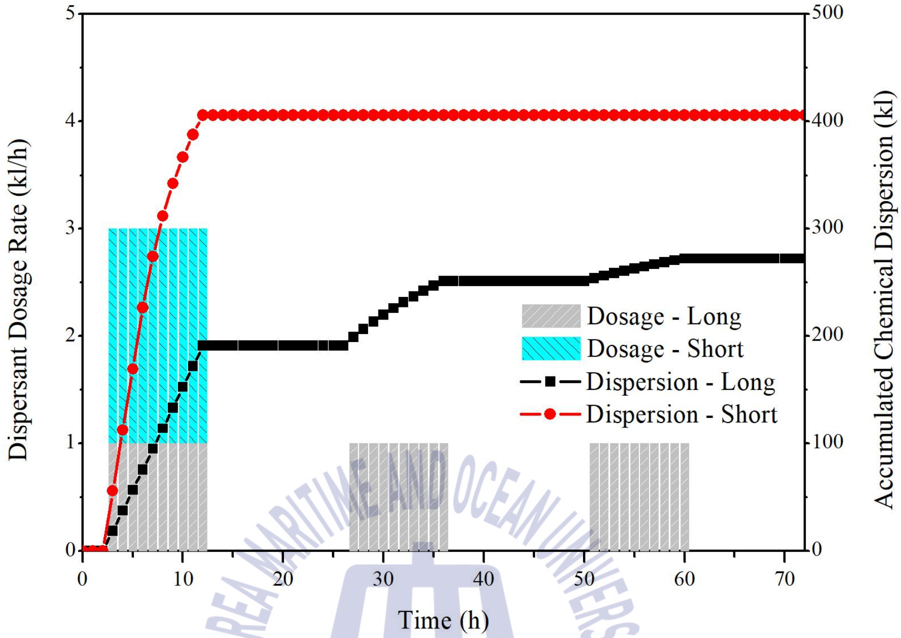

Fig. 9 Cumulative chemically dispersed oil volume and dispersant dosage rate according to dosage period (high dispersant efficiency) (Choe, et al., 2018)

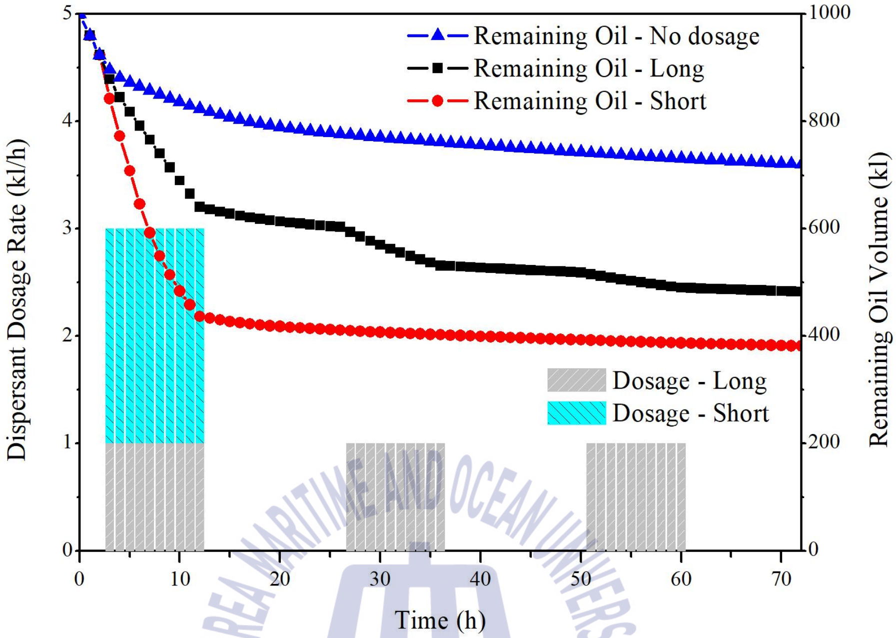

Fig. 10 Remaining oil volume and dispersant dosage rate according to dosage period (high dispersant efficiency) (Choe, et al., 2018)

The results of the sensitivity analysis showed that the dispersion efficiency of dispersant tends to be lowered due to change in properties of oil by weathering. Therefore, even if total amount of dispersant is the same, it can be understood that it is faster and more oil can be reduced to respond positively at the beginning of the accident than to respond it persistingly for a long time.

2.3 Estimation of the amount of chemical dispersion utilizing actual accident

Hebei Spirit oil pollution accident was selected as a test case in order to estimate the amount of chemical dispersion for actual accident cases using the developed calculation model. Oil information and environmental conditions were applied by using information of Hebei Spirit oil spill. 12,547 *kl* of Iranian Heavy was spilled at 7 a.m. Wind speed is 7~12 m/s for each day and water temperature is 12 ℃ by applying sea conditions at the time of accident. It is assumed that only dispersant is used for the response and used dispersant was Corexit 9527. Average values between high efficiency and low efficiency in Figs. 2 and 3 are applied to calculation. Considering decision-making time and distance to the point of accident, it is assumed that using dispersant starts after 6 hours from the accident and spraying dispersant proceeds until sunset. Simulation period is total 15 days. On the first day of the accident, middle and large-scale response vessels of central regional headquarters Korea coast guard spray dispersant. On the second day, response vessels of central and west regional headquarters Korea coast guard are mobilized. And from the third day, those of central, west and south regional headquarters Korea coast guard are mobilized. The calculation conditions for estimating the amount of chemical dispersion using actual accident cases are summarized in Table 6.

Table 6 Calculation conditions for estimating the amount of chemical dispersion of actual accident case (Choe, et al., 2018)

Oil	Iranian Heavy
° API	30
Viscosity	17 cSt @21 ℃
Spilled Volume	12,547 *kl*
Wind Speed	7~12 m/s
Water Temperature	12 ℃
Simulation Time	15 days
Application Speed	5 kn
DOR	0.05

Applying the above conditions, the cases were divided into the basic case ('Modified Hebei Spirit case') and the comparative case ('Dosage minimization case'). In the basic case, it is assumed that 300 *kl* of dispersant is used for 15 days, which is applied at the time of the Hebei Spirit oil pollution accident, and the amount of dispersant per hour is assumed to be constant. The comparative case means a calculation condition applying the smallest amount of dispersant required to obtain the same volume of chemical dispersion derived from calculation result of the basic case and this case was selected based on the sensitivity analyses. The other calculation conditions are the same as in the basic case, and there is a difference in that the dispersant rate changes per hour.

The calculations of the two cases were compared in Table 7 and Fig. 11. Table 7 shows the calculation results of the dispersant amount, chemical dispersion amount, evaporation amount, natural dispersion amount, and remaining oil amount of oil after 15 days of accidents. The natural evaporation amount is found to be larger than the comparative case in the basic case. The amount of evaporation increased largely at the beginning of the spill. The evaporation was less and the remaining amount was smaller in the comparative case because the initial amount of chemical dispersion through the dispersant was more. Since the amount of natural dispersion is relatively small, it is almost the same in both cases.

In the case of the basic case, spraying the dispersant was started from 6 hours after the accident, and 300 *kl* of dispersant was used for 15 days and a chemical dispersion amount of 625 *kl* was obtained. On the other hand, in the comparative case, it was calculated that the same chemical dispersion amount as that of the basic case can be obtained by spraying 105 *kl* for 5 hours from 6 hours after the accident. This shows that the spraying period of the dispersant is shorter than that of the basic case by 14 days, and the same chemical dispersion amount is obtained by using about 3 times less dosage amount.

Table 7 Result using actual accident information (Choe, et al., 2018)

Case	Basic	Best
Dispersant Dosage (*kl*)	300	105
Chemical Dispersion (*kl*)	625	
Evaporation (*kl*)	3,830	3,766
Natural Dispersion (*kl*)	13	13
Remaining Oil (*kl*)	8,079	8,143

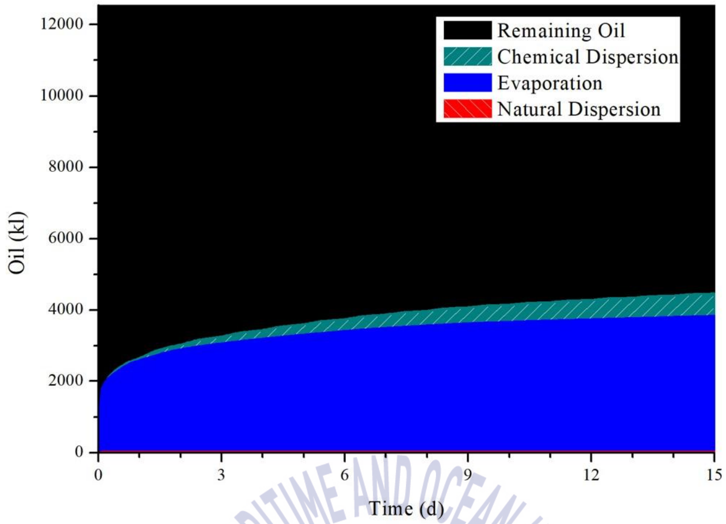

(a) Modified Hebei Spirit case

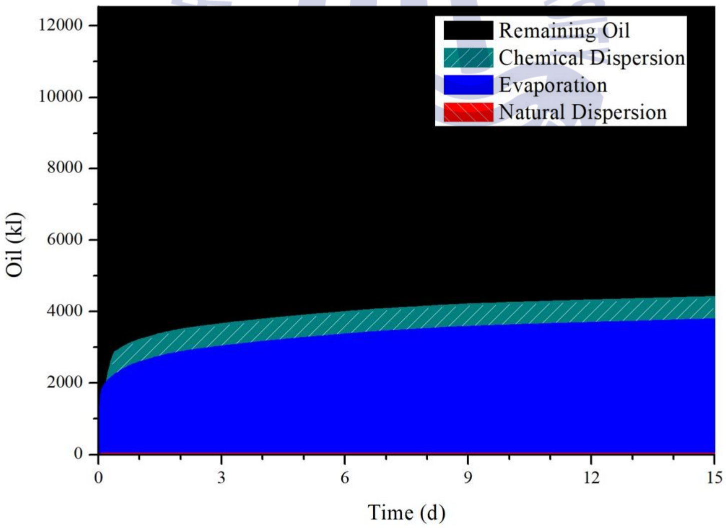

(b) Dosage minimization case

Fig. 11 Change of oil over time; (a) Modified Hebei Spirit case, (b) Dosage minimization case (Choe, et al., 2018)

Chapter 3 Estimation of the Mechanical Recovery Potential of Spilled Oil at Sea Considering the Spatial Thickness Distribution

3.1 Methods for estimating recovery potential

The recovery capacity calculation method considering the weathering, oil property, and equipment efficiency change were implemented in both spatially uniform model and spatially nonuniform model. The main difference between two models is that the spatially nonuniform model distinguishes the skimmed and the unskimmed zones in the oil slick and calculates the thickness variation of each zone separately.

3.1.1 Spatially uniform model

To calculate the recovery potential, the encounter rate (*ER*) of the emulsion, which is a mixture of oil and water, for a single skimmer can be obtained via Eq. (6) (Dale, 2011; BSEE & Genwest Systems, 2015):

$$ER = w * v * h_{em} * \Delta t \tag{6}$$

where w is the boom swath (m), v is the tow speed (m/s), and h_{em} is the thickness of the emulsion Δt is time step (3600 s).

The amount of recoverable encountered emulsion depends on the oil and sea conditions. The amount of recovered emulsion, emulsion recovery rate (*ERR*), in *ER* is determined by multiplying the throughput efficiency (*TE*) (BSEE & Genwest Systems, 2015). In addition, the oil recovery rate (*ORR*) can be determined by subtracting the amount of water from the amount of emulsion (Allen, et al., 2012):

$$ERR = ER^{*}\,TE \tag{7}$$

$$ORR = ERR^{*}(1-\Phi) \tag{8}$$

where *ERR* is the emulsion recovery rate, *TE* is the volume ratio of the recovered emulsion to the encountered emulsion and is a user-specified input, *ORR* is the oil recovery rate, and Φ is the water fraction in the emulsion.

Spatially uniform model considers oil type and sea conditions and calculates the oil area and weathering over time. Oil thickness is calculated every hour using Eq. (9). The emulsion thickness can be obtained by inserting (1-Φ) in the oil thickness equation:

$$h_{oil} = \frac{V}{A} \tag{9}$$

$$h_{em} = \frac{h_{oil}}{1-\Phi} \tag{10}$$

where h_{oil} is the average oil thickness, V is the remaining volume of oil on the sea surface, and A is the slick area.

The remaining oil volume over time is defined as the initial spilled volume minus the naturally removed volume and recovered volume from the start of spill until time t:

$$V(t) = V_0 - \sum_{0}^{t}(W(t) + ORR(t)) \tag{11}$$

The area of the oil slick is expressed as the product of characteristic lengths $l1$ and $l2$:

$$A(t) = l1 * l2 \tag{12}$$

where $l1$ is the spreading length under calm sea conditions, and $l2$ is the length increase due to spreading and wind (Galt, 2014).

In a calm sea, spreading undergoes three steps: an initial step, in which gravity and inertia are important (Eq. (13)); an intermediate step dominated by gravity and viscosity (Eq. (14)); and a final step during which surface tension and viscosity balance each other (Fay, 1969). The transition time from the intermediate step to the final step is approximately one week. Because this study focuses within the 72 hours after an accident, only the first two steps are considered, and the final step is excluded:

$$l1(t) = (V_0^{\frac{2}{3}} * t^2)^{\frac{1}{3}} \tag{13}$$

$$l1(t) = 0.01(100^{\frac{2}{3}} * V_0^{\frac{4}{27}} * t_0^{\frac{4}{9}} + 0.006(t - t_0))^{\frac{3}{2}} \tag{14}$$

where t is time in seconds. t_0 is the transition time from Eq. (13) to Eq. (14) and is a function of spilled volume, density, and viscosity.

After calculating spreading on a calm sea, the transport distance due to wind was considered assuming a constant wind direction. Movement by wind was assumed to occur at 3% of the wind velocity (Kinsman, 1965):

$$l2(t) = l1(t) + \int_0^t Z(t) \tag{15}$$

where $Z(t)$ is the distance that the oil slick has traveled due to wind at time t and $Z(t)$ is calculated by multiplying 0.03, wind speed, and time.

3.1.2 Spatially nonuniform model

This model applies spatial and temporal modifications to take account of the skimmed zone and oil thickness distribution. Applied methods and expected effects are described below. Concrete results using an accident scenario are detailed in Section 3.

3.1.2.1 Spatial improvements

When calculating the amount of recovered oil by the skimmers, studies of spatially uniform model have assumed that the recovered volume is a reduction in the total volume of the spilled oil slick as shown in Fig. 12a. The thickness of the total area decreases at the same rate across the whole oil slick because spatially uniform model studies assume that oil is recovered at the same rate in all areas. In uniform models that do not consider the spatial distribution of oil slick thickness, this thickness is used again in the recovery rate calculation. However, as shown in Fig. 12b, oil is recovered from only parts of the spill area rather than over the entire oil slick, and the actual oil slick thickness changes at different rates in skimmed areas and other areas. Therefore, the spatial variation in oil slick thickness should be considered, as the recovery potential of the skimmer is affected by the oil slick thickness as shown in Eq. (6).

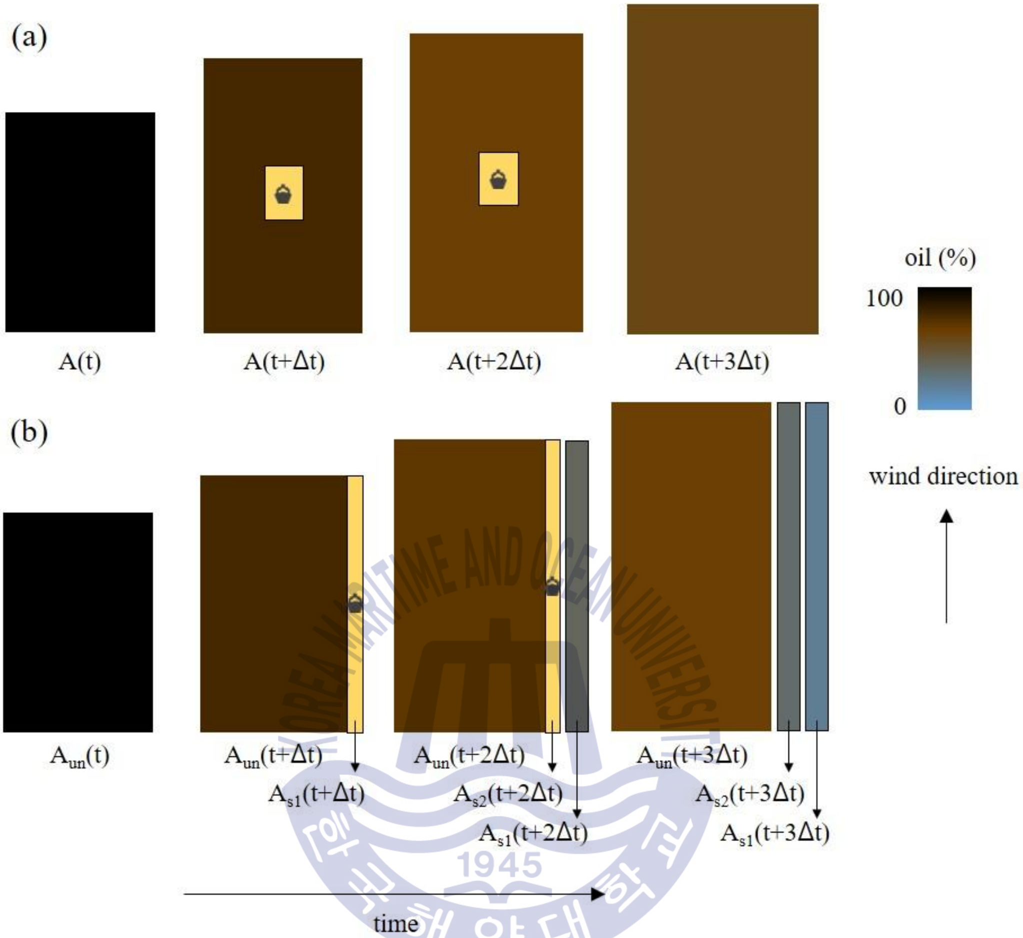

Fig. 12 Correlation between oil slick behavior and the skimming zone in (a) the spatially uniform model (b) the spatially nonuniform model. The yellow area represents a zone where skimming is in progress. A_{un}: area of the unskimmed zone; A_s: area of the skimmed zone (Choe, et al., under review)

Furthermore, spatially uniform model is limited in that it considers neither the space occupied by an individual skimmer in the spatial scope of oil slick nor the interactions between multiple skimmers. Thus, when calculating the response capacity using spatially uniform model, the amount of response resources (i.e., skimmers, etc.) applied to the oil slick area are essentially unlimited; spatially uniform models are allowed to apply the infinite quantity of response equipment units. However, there is a practical limit to the number of response resources that can be deployed to the limited size of an oil slick. Two spatial improvements are applied to the spatially nonuniform model to ameliorate these two limitations.

First, in order to distinguish spatial differences in thickness, we differentiated the skimmed and unskimmed zones herein; A_{un} denotes the area of the unskimmed zone and A_s denotes the area of the skimmed zone. Fig. 12a and Fig. 12b illustrate mechanisms from the spatially uniform model, and the spatially nonuniform model, respectively. As shown in Fig. 12a, the skimmed zone is not distinguished in the spatially uniform model. The spatially nonuniform model, however, distinguishes both zones as shown in Fig. 12b. The yellow section denotes a zone in which skimming is in progress at time *t*. The skimming zone at time t transforms into a skimmed zone at $t + \Delta t$. In other words, an area recovered by one skimmer becomes a skimmed zone in the next time step. The unrecovered oil among the encounter rate where the skimmer passed is regarded as remaining oil of skimmed zone. The amount of remaining emulsion in a skimmed zone equals *ER* minus *ERR* in Eq. (7), by the definition of *TE*. The legend in Fig. 12 shows the amount of oil remaining on the sea surface, which can also be thought of as the oil thickness.

The oil thickness in the skimmed zone can be represented differently from that in the unskimmed zone, because each zone is calculated separately. Furthermore, oil properties and behaviors such as weathering process including spreading phenomena are calculated separately in the unskimmed and skimmed zones; it is assumed that any oil recovery during the next time step occurs only in an unskimmed zone.

Second, to consider the space occupied by individual skimmers and interference between skimming systems, the area recovered by one skimming system and the quantity of skimming systems that can be deployed in the oil slick were computed and applied in the model.

To take advantage of the movement of oil due to wind during recovery, skimmers and oil booms are usually operated counter to the wind direction (Fingas, 2010). The spatially nonuniform model is thus programmed to recover oil in the *l2* direction. A_s, the area skimmed by a single skimming system in Δt, is calculated similar to the volume rate in Eq. (6), as shown in Eq. (16). Furthermore, because recovery is assumed to occur in the *l2* direction, the *l2* of the skimmed zone is identical to the *l2* of the entire oil slick. The *l1* length ($l1_s$) of the skimmed zone is defined by dividing the skimmed area A_s by *l2*:

$$A_s = w * v * \Delta t = l1_s * l2 \tag{16}$$

where $l1_s$ is the *l1* length of the skimmed zone. To prevent skimmer collisions, etc., a spatial margin is added as shown in Eq. (17). After this change, the area occupied by a single skimmer can be defined by Eq. (18):

$$A_{margin}(t) = l1_{margin}(t) * l2(t) \tag{17}$$

$$A_{occu}(t) = A_s(t) + A_{margin}(t) \tag{18}$$

where A_{occu} is the area occupied by a single skimming system and A_{margin} is the margin area, excluding the skimmed area, of a single skimming system. The full A_{occu} does not represent the recovered area, but it rather used to consider the interactions between skimmers. The recovered area A_s is equal to A_{occu} minus A_{margin}. $l1_{margin}$ is the margin length in the *l1* direction, which is assumed to be half of $l1_s$.

Finally, the maximum number of skimming systems, *x(t)*, that can be deployed in the unskimmed oil slick area at time *t* can be obtained via:

$$x(t) = \frac{A_{un}(t)}{A_{occu}(t)} \tag{19}$$

where A_{occu}(t) is the area covered by one skimming system at time t in Δt; Δt is 3600 s.

After oil recovery at time t, the $l1$ length of the unskimmed zone is updated via:

$$l1'_{un}(t) = l1_{un}(t) - l1_s(t) \tag{20}$$

where $l1'_{un}(t)$ is the $l1$ length of the unskimmed zone after skimming, and $l1_{un}$ is the $l1$ length of the unskimmed zone before recovery. If there is no skimming, $l1_s$ is zero and $l1'_{un}$ is equal to $l1_{un}$. To facilitate understanding, each space is illustrated in Fig. 13.

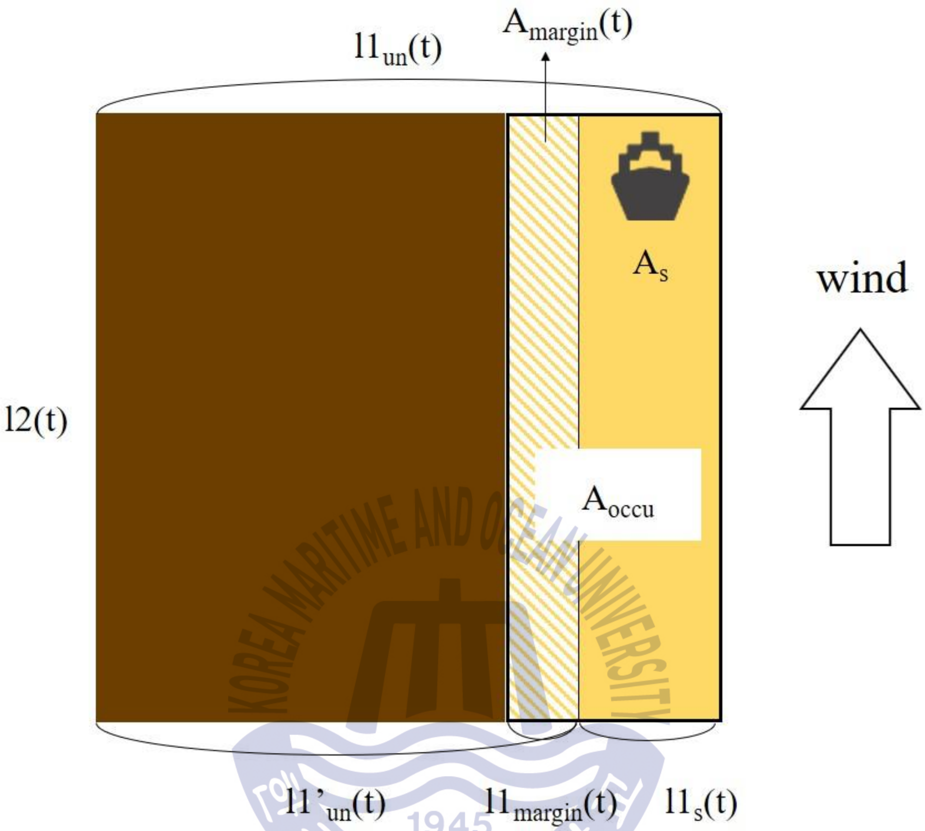

Fig. 13 Definitions of spaces used in the spatially nonuniform model (Choe, et al., under review)

As explained above, the spatially nonuniform model applies two spatial improvement methods. The first involves distinguishing between skimmed and unskimmed zones, and the second involves considering the space occupied by skimmers. In spatially uniform studies, differences in thickness were not spatially resolved due to oil recovery. The first improvement method allows the model to distinguish skimmed and unskimmed zones, which in turn facilitates the individual calculation of the area of and oil thickness in each zone. As a result, weathering is calculated differently for each zone as well. Thickness of the spatially uniform model and the spatially nonuniform model are illustrated in Fig. 14. The spatially uniform model assumes that oil is recovered at the same rate in all areas. On the other hand, the spatially nonuniform model supposes that encounter areas where the skimming systems pass are recovered only. Therefore, thickness in the spatially uniform model tends to be thinner than that of the unskimmed zone in the spatially nonuniform model. Furthermore, this figure shows the calculation result taken for one-hour recovery from 1h to 2h. The area that receives skimming changes from "unskimmed" to "skimmed" at 2 h as shown in Fig. 12b, because one skimmer responded beginning at 1 h. A total of two zones exist at 2 h in spatially nonuniform model and this recovered zone is thinner than the unskimmed zone. This zone can be computed separately from the unskimmed zone due to the improvement mentioned below.

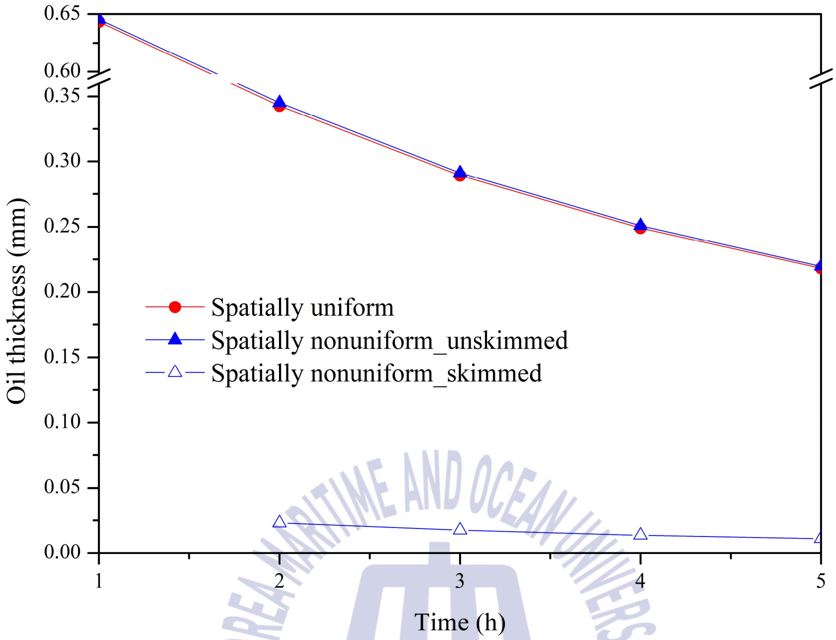

Fig. 14 Comparison between thickness of the spatially uniform model and spatially nonuniform model; effect of distinguishing between skimmed and unskimmed zones (Choe, et al., under review)

The second improvement allows the spatially nonuniform model to describe the space occupied by skimmers and prevent interference between them. The quantity of skimming systems that can be deployed is also calculated over time. In other words, the number of skimming systems that can be deployed is limited by considering interference between skimmers. Fig. 15 shows skimming systems number used the calculations and maximum number of skimming systems, *x(t)*, that can be deployed in the unskimmed oil slick of the spatially nonuniform model. In both of calculations, 30 skimming systems were entered as input value. This value is applied continuously in the calculation of the spatially uniform model. The quantity of skimming systems is 30 until 9 h in the spatially nonuniform model. But, this value drops from 10 h in the spatially nonuniform model as the maximum quantity of applicable skimming systems decreases below 30. That is to say, the spatially nonuniform model can consider the space occupied by an individual skimming system and the interactions between multiple skimming systems. These improvements allow the model to better reflect actual conditions.

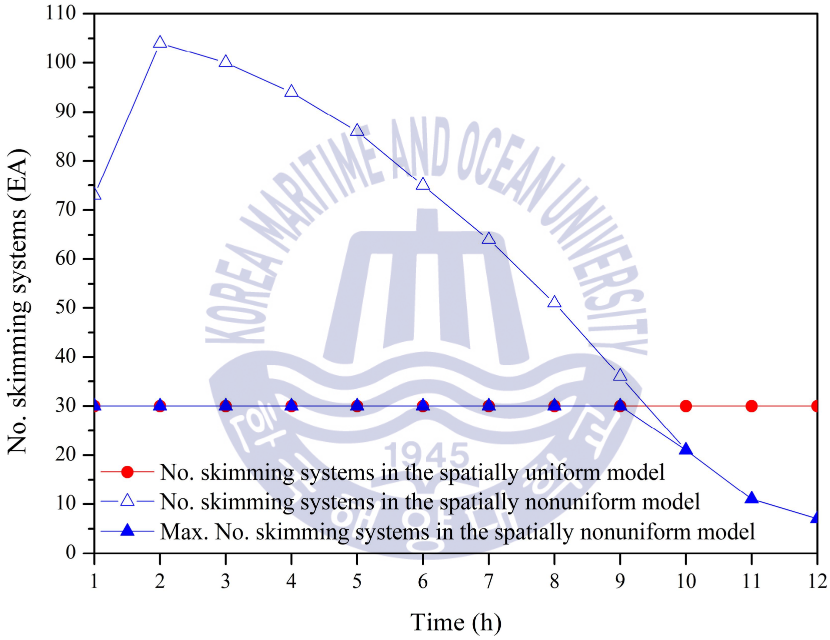

Fig. 15 Comparison of skimming systems quantity applied in the calculation and the maximum quantity of skimming systems, *x(t)*, with time in the spatially nonuniform model; effect of considering the space occupied by an individual skimming system and the interactions between multiple skimming systems (Choe, et al., under review)

3.1.2.2 Temporal improvement

Oil spreading is a function of the remaining oil volume and time, and calculations of oil properties, weathering, and skimmer recovery are performed at every time-step. The oil volume changes continuously with time due to weathering and clean-up activities such as mechanical recovery. Weathering is a function of area (i.e., weathering may increase or decrease with the area). However, the spatially uniform model doesn't reflect changes in oil volume in calculations of spreading area as shown in Eqs. (13) and (14).

The spatially nonuniform model uses a remaining volume that changes continuously, instead of the initial spill volume, to reflect the changes in oil slick volume over time when calculating spreading. Eqs. (13) and (14) in the spatially uniform model thus have been modified to Eqs. (21) and (22) in the spatially nonuniform model:

$$l1(t) = (V(t)^{\frac{2}{3}} * t^2)^{\frac{1}{3}} \tag{21}$$

$$l1(t) = 0.01(100^{\frac{2}{3}} * V^{\frac{4}{27}} * t_0^{\frac{4}{9}} + 0.006(t - t_0))^{\frac{3}{2}} \tag{22}$$

where *V(t)* is changed by weathering processes, such as oil evaporation and oil dispersion, and recovery, as in Eq. (11).

Next, the area change over time must be calculated separately in each zone because the skimmed zone and unskimmed zone are distinguished by the spatial improvement. The $l1$ of the unskimmed zone has been updated to $l1'_{un}$ as in Eq. (20). The $l1_{un}(t + \Delta t)$ is defined by adding the increase by spreading and wind, $\Delta l1$, to the length $l1'_{un}(t)$:

$$l1_{un}(t + \Delta t) = l1'_{un}(t) + \Delta l1_{un}(\Delta t) \tag{23}$$

where $\Delta l1_{un}(\Delta t)$ is the difference between the two $l1_{un}$ values calculated at time t and $t + \Delta t$ in Eqs. (21) or (22) and can be interpreted as the length increase due to spreading.

Likewise, the $l1$ of the skimmed zone at $t + \Delta t$ is also calculated as the sum of $\Delta l1_s$ and the $l1_s(t)$ at the previous time step. The $l1_s(t)$ value is obtained by dividing the skimmed area A_s by $l2$ as in Eq. (16), and the spreading at this value is:

$$l1_s(t+\Delta t) = l1_s(t) + \Delta l1_s(\Delta t) \tag{24}$$

The entire change in the length of $l1$ during Δt (from t to $t + \Delta t$), $\Delta l1_{entire}(\Delta t)$, is equal to the increase in length due to the total spreading in the unskimmed and skimmed zones:

$$\Delta l1_{entire}(\Delta t) = \Delta l1_{un}(\Delta t) + \Delta l1_s(\Delta t) \tag{25}$$

The $l2$ lengths of the unskimmed and skimmed zones can be calculated using the same equation. As shown in Eq. (15), $l2$ is defined as the length added due to wind to $l1$, which is the length considering spreading. Therefore, the spreading length $\Delta l1$ in Δt is added to the length at the previous time step, $l2(t)$, and the increase in length due to wind, ΔZ, is also added:

$$l2(t+\Delta t) = l2(t) + \Delta l1(\Delta t) + \Delta Z(\Delta t) \tag{26}$$

In Eqs. (21) and (22), which reflect the volume change over time, the area increase due to spreading is reduced in comparison to Eqs. (13) and (14) from the spatially uniform model. Area comparison between two models is shown in Fig. 16 for no recovery. The area of the unskimmed zone, assumed to be where recovery occurs in the spatially nonuniform model, is smaller than the spatially uniform model area. Thus, thickness of the spatially nonuniform model is thicker than that of the spatially uniform model.

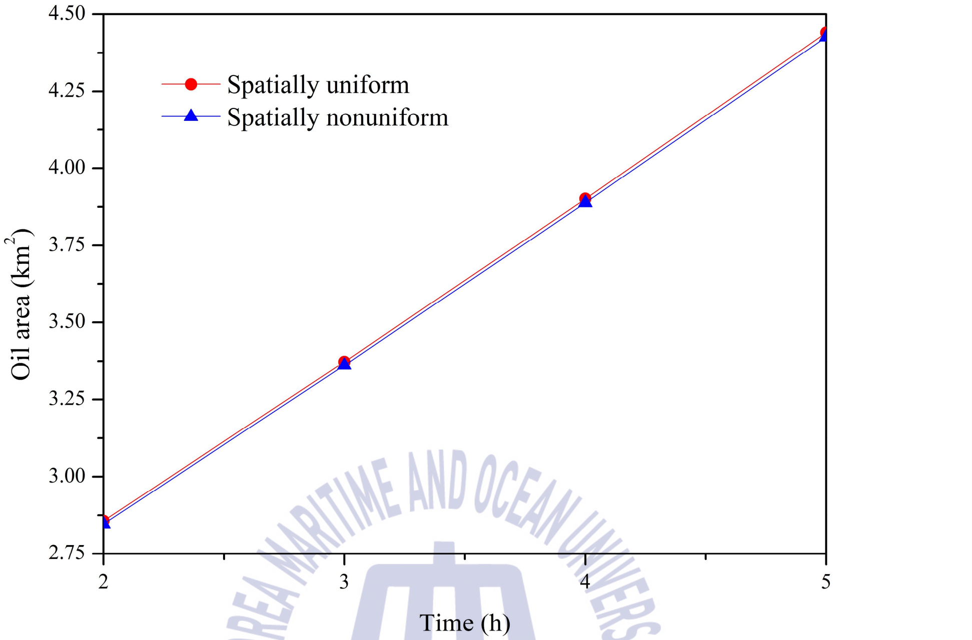

Fig. 16 Area comparison between the spatially uniform model and the spatially nonuniform model; difference in effect reflecting thickness distribution (Choe, et al., under review)

Furthermore, it is possible to calculate the areas of the skimmed and unskimmed zones separately described above, using the volume of remaining oil instead of the initial spill amount. As a result, the area changes in the skimmed and unskimmed zones show different trends. In order to separately calculate the skimmed and unskimmed zone areas, the unskimmed zone is defined as the area remaining outside the skimmed zone and spreading of unskimmed zone during the next time step is calculated in this area. Therefore, if the skimmed area to be excluded becomes larger than the area increased due to spreading and wind at time t, the area of the unskimmed zone at $t + \Delta t$ decreases. On the other hand, if the area increased due to spreading and wind is larger, the area of the unskimmed zone will increase.

3.2 Results

3.2.1 Comparison of calculation results using a virtual accident scenario

In this section, calculation results performed using two models (spatially uniform model, and spatially nonuniform model) are compared and analyzed. The scenario was created to compare two models; the inputs used for the calculations are listed in Table 8. In this scenario, 500 *kl* of Bunker C oil had been spilled in the sea of Busan, Republic of Korea. The simulation time is 24 hours after the accident. All 20 skimming systems are applied from 1 h to 24 h. The 3-yr average wind velocity and water temperature in the Busan area between 2014 and 2016 were used. Information of Transrec 100 skimmer, which are deployed on response vessel Chungryong 108, was used in the simulation. A *TE* of 50% was applied. Recovery efficiency (RE), which is defined as the percent of emulsion excluding water in the total recovered volume, was calculated over time. The size of the storage tank is assumed to be large enough to exclude time for emptying the storage tank.

Table 8 Scenario and input values in the model comparison (Choe, et al., under review)

Oil spill scenario		Input values
Spilled amount (*kl*)		500
Oil type		Bunker C fuel oil
Wind speed (m/s)		4.4
Water temperature (° C)		16.8
Skimming system		Chungryong 108 and Transrec 100 information were used.
Efficiency	TE	50%
	RE	Time-based calculation
Operation time		1 h after accident – 72 h after accident

The spatially uniform model considers reduction by both recovery and weathering, which includes evaporation and natural dispersion. The spatially nonuniform model not only considers removal by recovery and weathering, but also assumes that thin slicks (with a thickness of less than 0.6 μm) have been removed, as such slicks dissipate naturally from a response viewpoint (ITOPF, 2011; FIngas, 2016). As shown in Fig. 17, the spatially nonuniform model shows a total removal of 452 *kl* of oil during 24 h due to three mechanisms, namely mechanical recovery, weathering, and dissipation due to exceptionally low thickness. Of this, 54% is due to recovery, 7% is due to weathering, and 39% is due to dissipation. Dissipation accounts for 39% of the total at 24 h, while there was no oil dissipation at 12 h. This can be explained by the thin skimmed zone generated from 17 h onward, which has a thickness of less than 0.6 μm. For example, 80 skimmed zones have a thickness of less 0.6 μm at 17 h, and the total volume of these 80 zones is approximately 29.7 *kl*. The total oil volume removed by dissipation during 24 h is 178 *kl* with 347 skimmed zones and 20 skimmed zones are left. The same criteria were applied to the spatially uniform model. But no reduction in thickness to less than 0.6 μm is observed, as oil decreases over the whole oil slick body rather than in specific areas. The spatially uniform model shows a total removal of 251 *kl* of oil during 24 h due to two mechanisms. Of this, 230 *kl* is due to recovery, 21 *kl* is due to weathering.

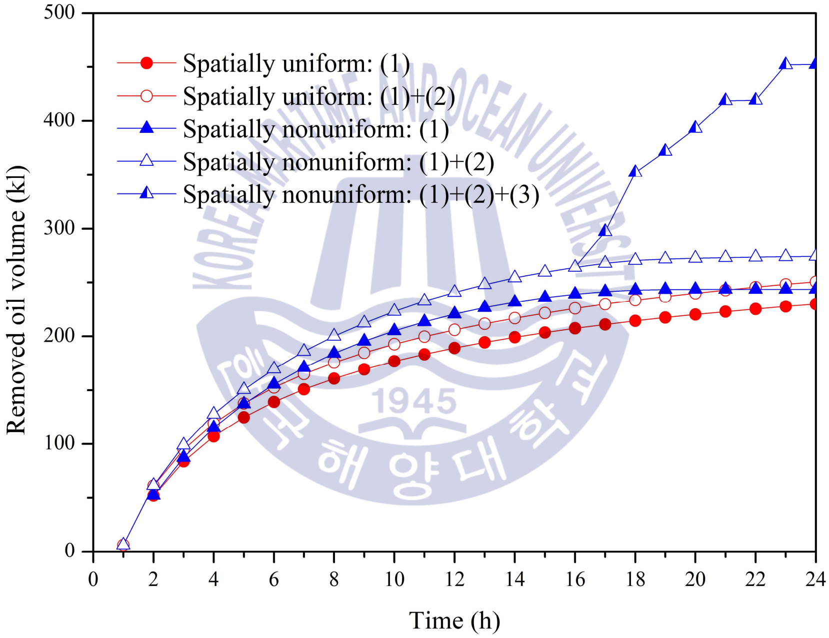

Fig. 17 Comparison of cumulative volume of removed oil between the spatially uniform model and the spatially nonuniform model: (1) volume of oil recovered by the skimmer, (2) volume removed by weathering, (3) volume dissipated by thin slicks with an oil thickness of less than 0.6 μm (Choe, et al., under review)

Fig. 18 shows the quantity of skimming systems used in the spatially nonuniform model calculation and the quantity of skimmed zones over time. Twenty skimming systems begin response 1 h after the accident. Hence 20 skimmed zones and one unskimmed zone exist at 2 h. Likewise, 20 skimmed zones appear again due to recovery efforts beginning at 2 h, leaving 40 skimmed zones and 1 unskimmed zone at 3 h. In this way, the zones recovered at time t are converted to skimmed zones at $t + \Delta t$ and calculated separately from the unskimmed zone. Twenty skimmed zones are newly generated at 17 h, because 20 skimmers were operational at 16 h. At the same time, however, 80 of the existing skimmed zones dissipate due to reduced thickness (i.e., < 0.6 μm). Therefore, the number of skimmed zones decreases by 60 at 17 h compared to that at 16 h. The thickness of the unskimmed zone is reduced to less than 0.6 μm at 21 h (Fig. 20), and no further oil is recovered. As a result, no more skimmed zones are generated. The number of skimming systems applied is initially constant at 20, but then drops below 20 beginning at 17 h, as the number of skimming systems that can be deployed decrease with the unskimmed area (Fig. 19). The size of the unskimmed zone (where skimmers can operate) can be grasped in the spatially nonuniform model, as the model takes into account the space occupied by skimming systems and distinguishes unskimmed and skimmed zones to consider spatial changes in thickness. Therefore, the maximum number of deployable skimming systems can be also derived at a given time. In contrast, spatially uniform model does not explore the maximum number of deployable skimming systems, so 20 skimmers which were initially entered are applied continuously in the calculations; spatial differences cannot be distinguished, either.

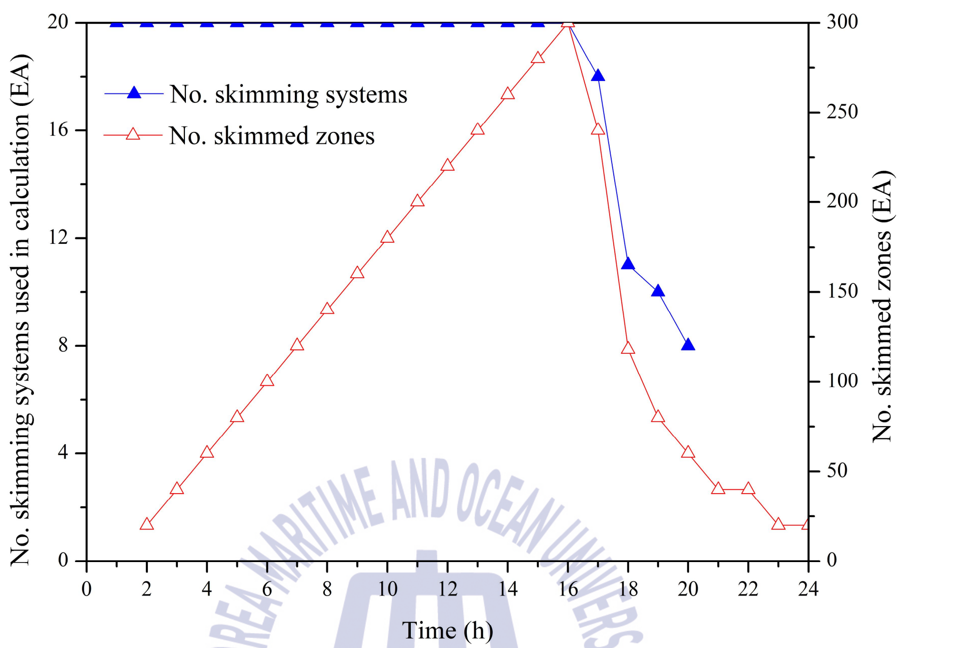

Fig. 18 Number of skimming systems used in the calculation and the number of skimmed zones with time in the spatially nonuniform model (Choe, et al., under review)

Fig. 19 illustrates the spatially uniform model oil slick area and the unskimmed zone in the spatially nonuniform model. In spatially uniform model, the oil slick area is calculated as a function of the initial spill volume as in Eqs. (13) and (14), and it continuously increases without reflecting changes in volume. In contrast, it is possible to reflect volume changes since the spatially nonuniform model distinguishes skimmed and unskimmed zones as described above. As the volume continuously decreases and the unskimmed zone transits to skimmed zones beginning at 2 h by oil recovery, the unskimmed area is always smaller than the spatially uniform model area. Furthermore, area decreases can be seen in the unskimmed area from 6 h to 20 h. It is because the area converted from unskimmed to skimmed is larger than the area increases of unskimmed zone due to spreading and wind during this time.

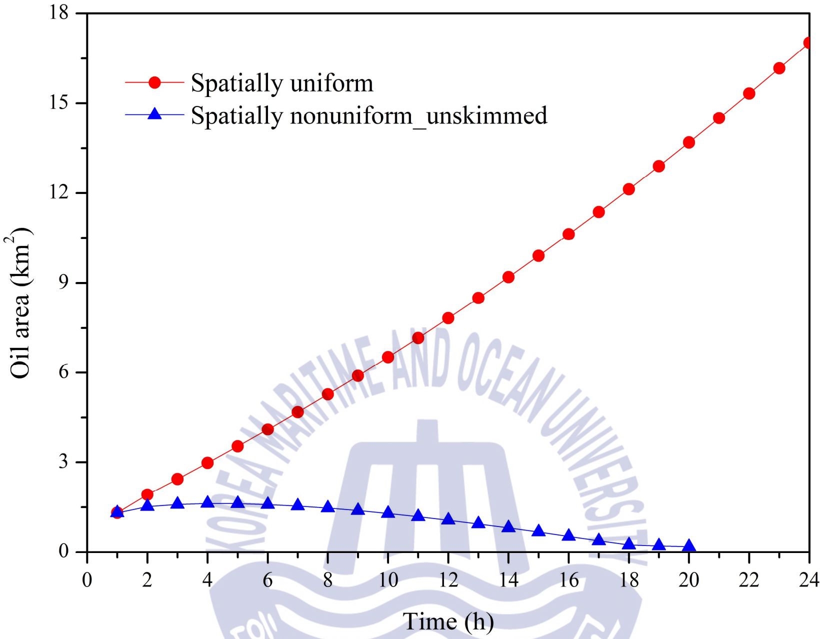

Fig. 19 Comparison between the spatially uniform model oil slick area and the unskimmed zone area of the spatially nonuniform model (Choe, et al., under review)

The thickness of the unskimmed zone in the spatially nonuniform model can be seen in Fig. 20. In spatially uniform model, the volume decreases due to oil recovery at the same rate in all zones with no spatial distinction. In contrast, the spatially nonuniform model distinguishes skimmed zones that have become thin due to oil recovery from the unskimmed zone. Therefore, the thickness of the unskimmed zone is not directly affected by the removed amount in the spatially nonuniform model. If there no recovery activity is undertaken, no zones are converted into skimmed zones. Then II_s in Eq. (20)

becomes zero and the difference between $l1$ values from the spatially uniform model and $l1_{un}$ from the spatially nonuniform model appears by only Eqs. (21) and (22). Because volume decrease over time is reflected in these equations, the $l1_{un}$ and area in the spatially nonuniform model are smaller than the $l1$ and area in the spatially uniform model as Fig. 16. As a result, the thickness of the unskimmed zone in the spatially nonuniform model becomes thicker than that in the spatially uniform model. However, the oil remaining in the unskimmed zone decreases to a smaller amount and the thickness is also reduced, as recovery progresses and unskimmed zone is converted into skimmed zones. At 21 h, the unskimmed zone dissipates as its thickness decreases below 0.6 μm, and weathering and recovery of that are no longer calculated.

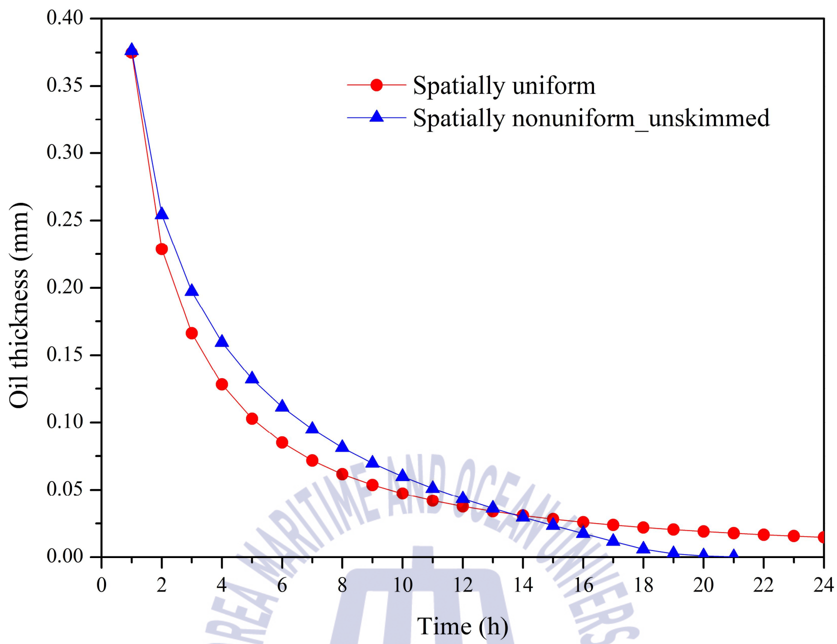

Fig. 20 Comparison of oil thickness in the spatially uniform model and the spatially nonuniform model for 24 h (Choe, et al., under review)

Fig. 21 shows oil recovery rate and cumulative recovery volume. The recovery rate features a trend similar to thickness, and the oil recovery rate is larger in the spatially nonuniform model than in the spatially uniform model until 14 h. However, the recovery rate of the spatially nonuniform model is smaller than that of the spatially uniform model beginning at 15 h result from reduced thickness in the spatially nonuniform model from 14 h. The amount of oil recovered in 24 h is 230 *kl* in spatially uniform model and 243 *kl* in the spatially nonuniform model. Recovery volume of spatially nonuniform model the is higher by 24 *kl* than that of spatially uniform model, despite the smaller quantity of skimming systems applied from 17 h onward.

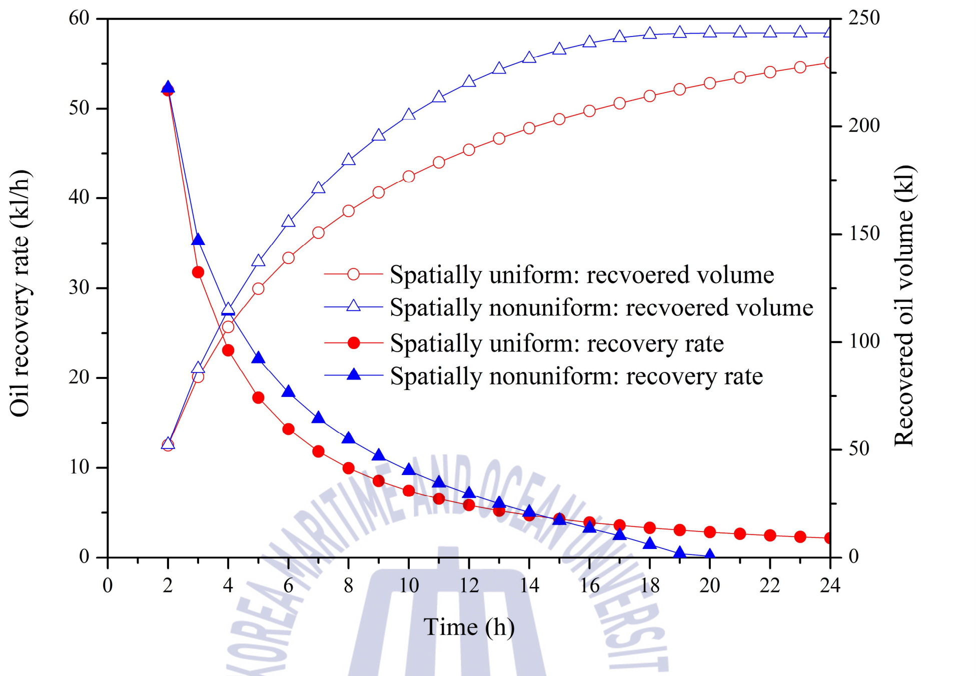

Fig. 21 Comparison of oil recovery rate and cumulative recovery volume between the spatially uniform model and the spatially nonuniform model (Choe, et al., under review)

The volume of remaining oil on the sea surface over 24 h is illustrated in Fig. 22. The total volume of spatially nonuniform model is equal to the sum of unskimmed and all skimmed zones with a thickness of 0.6 μm or larger. The amount of oil remaining (compared to the initial spilled volume of 500 *kl*) is 50% in spatially uniform model and 10% in the spatially nonuniform model at 24 h. However, the recovered volume of the spatially nonuniform model is calculated using less than 20 skimmers from 17 h onward. Therefore, to enable comparison of recovery time rather than volume, half of the initial spilled volume, 250 *kl*, is indicated in Fig. 22. It took 24 h and 14 h, for the volume of remaining oil in spatially uniform model and the spatially nonuniform model respectively to reach half of the initially spilled volume. Thus, less time was required to remove half of the initial spilled volume in the spatially nonuniform model.

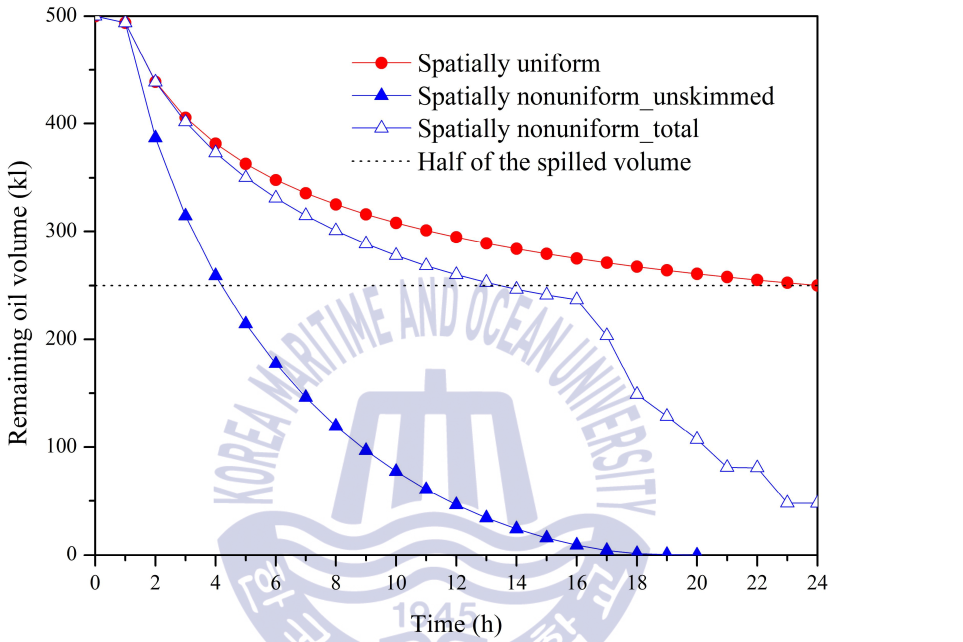

Fig. 22 Comparison of remaining oil volume of the spatially uniform model and unskimmed zone, total zone in the spatially nonuniform model, and half of the spill (Choe, et al., under review)

3.2.2 Comparison of calculation results using a actual accident information

The calculation was performed using the information of the actual accident through two models; the inputs used for the calculations are listed in Table 9. In this scenario, 900 *kl* of Basrah light oil had been spilled. The simulation time is 72 hours after the accident. Information of Normar 200TI skimmer, which are deployed on response vessel Hwangryong 208, was used in the simulation. All 10 skimming systems are applied from 1 h to 72 h. The size of the storage tank is assumed to be large enough to exclude time for emptying the storage tank.

Table 9 Input values using actual accident information

Oil spill scenario	Input values
Spilled amount (*kl*)	900
Oil type	Basrah light
Wind speed (m/s)	8
Water temperature (℃)	13.5
Skimming system	Hwangryong 208 and Normar 200TI information were used. 10 of skimming systems were mobilized.
Skimmer performance	Time-based calculation
Operation time	1 h after accident - 72 h after accident

The volume of remaining oil on the sea surface over 72 h is illustrated in Fig. 23. The amount of oil remaining in the spatially nonuniform model are 390 *kl* after 72 hours and 494 *kl* in the spatially uniform model. Recovered oil volume are 97 *kl* and 109 *kl* for the spatially uniform model and the spatially nonuniform model, respectively. The volume of naturally dissipated oil is 97 *kl* in the spatially nonuniform model.

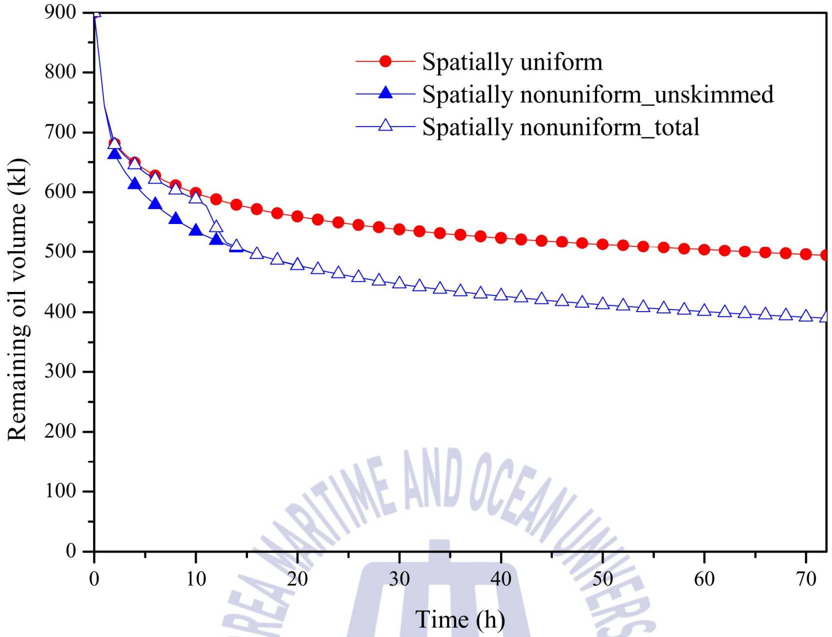

Fig. 23 Comparison of remaining oil volume of the spatially uniform model and unskimmed zone and total zone in the spatially nonuniform model

Finally, Table 10 shows number of skimming systems required to recover all residual oil. About 34 skimming systems were mobilized in the actual accident (Kim, et al., 2018) and this value was found to be closer to the spatially nonuniform model.

Table 10 comparison of result using actual accident information

Case	Spatially uniform model	Spatially nonuniform model	Actual accident (Kim, et al., 2018)
No. skimming systems	95	31	34

Chapter 4 Conclusions

4.1 Analysis of Estimation of chemical dispersion amount considering the dispersant dosage and change of oil properties by weathering

Dispersant can be used under conditions where mechanical recovery is difficult and it is recognized as effective control means capable of rapidly processing large areas. However, the toxicity of crude oil, dispersant, and chemically dispersed oil can have a impact on marine life. Most countries apply restrictively dispersant due to the negative effects although the usefulness of dispersant has been proven. Therefore, in order to mitigate negative concerns, it would be very useful to reduce the application amount of dispersant while obtaining the same dispersion effect. It is necessary to understand the quantitative correlation between the dispersant amount and the amount of chemical dispersion. However, researches that can quantitatively analyze the correlation between dispersant amount and the amount of residual oil on the sea and utilize it for the response strategy are very insufficient. The amount of chemical dispersion also varies depending on the timing of the use of dispersant, since the characteristics of the spilled oil are continuously changed by weathering effects in case of oil spill in the sea.

The calculation algorithm considering oil property change due to weathering was developed and sensitivity studies were conducted to estimate the chemical dispersion amount according to the dispersant dosage and spraying period, at the same time considering the weathering effects. Also, Hebei Spirit oil pollution accident was selected as a test case in order to estimate the amount of chemical dispersion for actual accident cases using the developed calculation model. The basic case which applies information on dosage period and amount at the time of the Hebei Spirit oil pollution accident and the comparative case means a calculation condition applying the smallest amount of dispersant required to obtain the same volume of chemical dispersion derived from calculation result of the basic case were calculated and compared. Conclusions of this study are as follows.

The dispersion efficiency of dispersant is affected by wind speed and viscosity. Oil evaporates and emulsifies over time, resulting in higher viscosity. It was found that dispersion efficiency of the dispersant is lowered with time since oil does not disperse well even when dispersant is used. Thus, it is faster and more oil can be reduced to respond positively at the beginning of the accident than to respond it persistingly for a long time. Therefore, when sufficient dispersant is used at the beginning of the accident, the same amount of chemical dispersion can be obtained even with a smaller amount of dispersant.

In the case of the basic case, spraying the dispersant was started from 6 hours after the accident, and 300 *kl* of dispersant was used for 15 days and a chemical dispersion amount of 625 *kl* was obtained. On the other hand, in the comparative case, which is derived from sensitivity studies, it was calculated that the same chemical dispersion amount as that of the basic case can be obtained by spraying 105 *kl* for 5 hours. This means that in the case of increasing the amount of dispersant used at the beginning of the accident, the same volume of chemical dispersion was obtained, while the dosage period of the dispersant was shortened by 14 days and reducing the dosage amount by three times.

The quantitative correlation between the amount of the dispersant and the remaining oil on the sea derived from this study will be useful in establishing the response strategy using the dispersant. It is meaningful that dosage period and amount of the dispersant can be minimized to obtain the same chemical dispersing effect and at the same time the concern about the toxic effect due to the spraying the dispersant can be reduced. If related data on domestic dispersant are secured in the future, it will be possible to conduct research using them.

4.2 Estimation of the Mechanical Recovery Potential of Spilled Oil at Sea Considering the Spatial Thickness Distribution

Numerous studies have been conducted to predict recovery potential and establish response strategies for oil spill accidents at sea. However, researches remain insufficient on recovery potential estimation methods that consider weathering, oil properties, and equipment efficiency. General studies considered all of these factors can't distinguish difference between recovered region and non-recovered region. Two models were developed in this study. One is spatially uniform model which doesn't consider skimmed zone and thickness distribution and the other is model considering skimmed zone and thickness distribution (spatially nonuniform model). Three improvements that allow the model to better reflect actual conditions, were applied to the spatially nonuniform model. Calculation of two models were conducted through the virtual accident scenario to compare the effects of considering the thickness distribution between skimmed and unskimmed zones. The recovery potential and its effects on the responses were compared and analyzed. Improvements methods applied to the spatially nonuniform model, and the effects of these features are described below.

First, spatially uniform studies are limited in that all oil had the same thickness and are considered a single oil slick, with no spatial variations in thickness. The first improvement in the spatially nonuniform model considers these spatial changes in thickness by distinguishing areas where oil recovery was performed from those where it was not. Through this change, a more realistic recovery volume can be calculated using the thickness of each zone; the area of and weathering in each zone can also be calculated. This zone distinction in the spatially nonuniform model allowed the model to represent thin slicks, which could not be distinguished in the spatially uniform model, and reflect natural oil dissipation effects. In the calculation result through the spatially nonuniform model, a total of 367 skimmed zones were generated. 347 zones of total skimmed zones and the unskimmed zone with thin thickness dissipated during 24 h, leaving 20 skimmed zones at 24 h.

Second, spatially uniform models don't take into account neither the space occupied by a single skimmer nor spatial inference with other skimmers. Therefore, any quantity of skimming systems could be applied by the user in the calculations with no spatial constraints. The second improvement of the spatially nonuniform model involved the calculation of both the space occupied by a skimmer and the interactions between skimmers. This allowed the model to estimate the maximum applicable number of skimming systems over time and apply this number in the recovery potential calculation. The unskimmed area in the calculation of spatially nonuniform model decreased over time. As a result, the actual quantity of deployable skimming systems also decreased, and this decrease was reflected in the recovery volume calculation, which applied less than 20 skimming systems from 17 h onward. The upper limit to the number of skimming systems used depends on the oil area, and thus the number of skimming systems applied in the calculation changes with the oil area. This enables the application of more realistic quantities of available skimming systems in the model.

Third, spatially uniform studies calculate oil spreading using the initial spill volume, and changes in the residual oil volume due to weathering processes (such as evaporation and natural dissipation) and mechanical recovery were not considered. This must be corrected, as oil volume and area are important factors in recovery rate calculations. The third improvement applied in the spatially nonuniform model involved application of residual oil volume changes the at the sea surface with time. Furthermore, this enables area calculations of each zone by using the volume of each zone.

The calculation comparing the spatially nonuniform model which is applied its three improvements with the spatially uniform model revealed the following results. The total recovered oil volume was 230 *kl* in the spatially uniform model and 243 *kl* in the spatially nonuniform model during 24 h. Finally, 50% and 10% of the initially spilled volume remained in the spatially uniform and nonuniform models, respectively. Furthermore, it took 24 h and 14 h for the volume of remaining oil in the spatially uniform and nonuniform models respectively to reach half of the initially spilled volume. Thus, less time was required to remove half of the initially spilled volume in the spatially nonuniform model. Moreover, the spatially nonuniform model calculated the recovery potential using less than 20 skimmers from 17 h onward due to potential interference between skimmers. Thus, in order to recover more oil, the spatially uniform model can apply more skimmers (which is unrealistic, as skimmers may interfere with each other). On the other hand, if the oil recovery systems exceed the oil slick size, the spatially nonuniform model must perform oil recovery for a longer period of time.

Even though the spatially nonuniform model in this study does not perfectly reflect all conditions seen in actual accidents, it can allow a greater understanding of trends in spilled oil behavior after the application of mechanical skimmers and be used for preparedness and response in the event of oil spills at sea. Regarding accident preparedness, this model can be utilized to estimate and reserve the required response resources in the event of oil spill accidents. Regarding accident response, specific accident information can be applied in this model, and the trends presented by the model can be utilized to make decisions such as when, how many, and what skimmers to deploy.

References

Allen, A.A. & Dale D.H., 1995, Dispersant mission planner: A computerized model for the application of chemical dispersants on oil spills, *in proc. of 18th AMOP Technical Seminar*, Environment Canada, pp.393-414.

Allen, A., Dean, D., Galt, J. & Murphy, J., 2012. EDRC Project Final Report. Edmonds, WA.

Almeda, R., Hyatt, C. & Buskey, E.J., 2014. Toxicity of dispersant Corexit 9500A and crude oil to marine microzooplankton. Ecotoxicol. *Environ. Saf.*, 106, pp.76-85. https://doi.org/10.1016/j.ecoenv.2014.04.028

Almeda, R., Wambaugh, Z., Wang, Z., Hyatt, C., Liu, Z. & Buskey, E.J., 2013. Interactions between Zooplankton and Crude Oil: Toxic Effects and Bioaccumulation of Polycyclic Aromatic Hydrocarbons. *PLoS One*, 8. https://doi.org/10.1371/journal.pone.0067212

Antoine, C., 1888. Vapor Pressure: a new relationship between pressure and temperature. *CR Acad Sci*, 107, pp.681-685.

American Society for Testing and Materials (ASTM), 2015. F1737 Standard Guide for Use of Oil Spill Dispersant Application Equipment During Spill Response: Boom and Nozzle Systems. ASTM Int. https://doi.org/10.1520/F1737

American Society for Testing and Materials (ASTM), 2013. F2532 Standard Guide for Determining Net Environmental Benefit of Dispersant Use. ASTM Int. https://doi.org/10.1520/F2532-13.2

Berry, A., Dabrowski, T. & Lyons, K., 2012. The oil spill model OILTRANS and its application to the Celtic Sea. *Mar. Pollut. Bull.*, 64, pp.2489-2501. https://doi.org/10.1016/j.marpolbul.2012.07.036

Bocard, C., Castaing, G. & Claude, G., 1984. Chemical oil dispersion in trials at sea and in laboratory tests: the key role of dilution processes, in: Allen, T.E. (Ed.), Oil Spill Chemical Dispersants: Research, Experience, and Recommendations. ASTM International, pp.125-142.

Brandvik, P.J., Lise, J., Resby, M., Snorre, P., Leirvik, F. & Fritt-rasmussen, J., 2010. Oil in ice - JIP Report No.19: Meso-scale weathering of oil as a function of ice conditions, Oil Properties, Dispersibility and In Situ Burnability of Weathered Oil as a Function of Time.

British Petroleum, 2017. BP Statistical Review of World Energy 2017, British Petroleum. London SW1Y 4PD, United Kingdom.

Bureau of Safety and Environmental Enforcement (BSEE) & Genwest Systems, 2015. Estimated Recovery System Potential (ERSP) Calculator User Manual.

Cho, H., Ha, C., 2012. The Effectiveness of the Dispersant Use during the "Deepwater Horizon" Incident -REVIEW of the Proceedings from 2011 International Oil Spill Conference-. *Korean Soc. Mar. Environ. Saf.*, 18, pp.61-65.

Choe, Y., Kim, H. & Huh, C., 2018. Estimation of Chemical Dispersion Amount Considering the Dosage of Dispersant and Change of Oil Properties by Weathering. *J. Korean Soc. Mar. Environ. Energy*, 21, pp.1-10. https://doi.org/https://doi.org/10.7846/JKOSMEE.2018.21.4.1

Choe, Y., Kim, H. & Huh, C., (under review). Estimation of the Mechanical Recovery Potential of Spilled Oil at Sea Considering the Spatial Thickness Distribution. *Environ. Manage.*

Cohen, J.H., McCormick, L.R. & Burkhardt, S.M., 2014. Effects of dispersant and oil on survival and swimming activity in a marine copepod. *Bull. Environ. Contam. Toxicol.*, 92, pp.381-387. https://doi.org/10.1007/s00128-013-1191-4

Daemyung Chemical, *ECO-CLEAN Dispersant* [Online] (Updated 8 January 2005) Available at:

http://www.daemyungchem.co.kr/shop/goods/goods_view.php?goodsno=293&category=006001, [Accessed 03 August 2018]

Dale, D., 2011. Response Options Calculator (ROC) - Users Guide.

Delvigne, G.A.L. & Sweeney, C.E., 1988. Natural dispersion of oil. *Oil Chem. Pollut.*, 4, pp.281-310. https://doi.org/10.1016/S0269-8579(88)80003-0

Eley, D.D., Hey, M.J. & Symonds, J.D., 1988. Emulsions of water in asphaltene-containing oils 1. Droplet size distribution and emulsification rates. *Colloids and Surfaces*, 32, pp.87-101. https://doi.org/10.1016/0166-6622(88)80006-4

Kim, H., Choe, Y. & Huh, C., 2018. A Study on the Improvement of Skimmer' s Recovery Capacity Estimation: Comparative Analysis with WuYiSan Oil Spill Case. *J. Korean Soc. Mar. Environ. Energy*, 21, pp.1-11. https://doi.org/https://doi.org/10.7846/JKOSMEE.2018.21.4.1

Environmental Protection Agency (EPA), *COREXIT® EC9527A*, [Online] (Updated 18 December 1995) Available at: http://www.epa.gov/emergency-response/corexitr-ec9527a, [Accessed 03 July 2018]

Fay, J.A., 1969. The spread of Oil Slick on a Calm Sea, in: Hoult, D.P. (Ed.), Oil on the Sea. Springer, Boston, MA, pp.53-63. https://doi.org/https://doi.org/10.1007/978-1-4684-9019-0

Fingas, M. & Fieldhouse, B., 2009. Studies on crude oil and petroleum product emulsions: Water resolution and rheology. *Colloids Surfaces A Physicochem. Eng. Asp.*, 333, pp.67-81. https://doi.org/10.1016/j.colsurfa.2008.09.029

Fingas, M., 2011. Oil Spill Science and Technology. Gulf Professional Publishing. https://doi.org/https://doi.org/10.1016/C2009-0-19703-9

Fingas, M., Fieldhouse, B., 2012. Studies on water-in-oil products from crude oils and petroleum products. *Mar. Pollut. Bull.*, 64, pp.272-283. https://doi.org/10.1016/j.marpolbul.2011.11.019

Fingas, M., 2016. Oil Spill Science and Technology. Gulf Professional Publishing. https://doi.org/https://doi.org/10.1016/C2015-0-04851-1

Galt, J.A., 2014. Oil Weathering Technical Documentation and Recommended Use Strategies.

Galt, J.A.A. & Overstreet, R., 2009. Development of Spreading Algorithms for the ROC, Response Options Calculator (ROC).

Goodbody-Gringley, G., Wetzel, D.L., Gillon, D., Pulster, E., Miller, A. & Ritchie, K.B., 2013. Toxicity of Deepwater Horizon Source Oil and the Chemical Dispersant, Corexit® 9500, to Coral Larvae. *PLoS One*, 8, pp.1-10. https://doi.org/10.1371/journal.pone.0045574

Hong, S., Khim, J.S., Ryu, J., Kang, S.G., Shim, W.J. & Yim, U.H., 2014. Environmental and ecological effects and recoveries after five years ofthe Hebei Spirit oil spill, Taean, Korea. *Ocean Coast. Manag.*, 102, pp.522-532. https://doi.org/10.1016/j.ocecoaman.2014.01.006

International Petroleum Industry Environmental Conservation Association (IPIECA) & International Association of Oil and Gas Producers (IOGP), 2015. *Oil spill preparedness and response: an introduction.*

International Tanker Owners Pollution Federation Limited (ITOPF), 2011. Aerial Observation of Marine Oil Spills. Tech. Inf. Pap. 12.

Jokuty, P., Fingas, M., Whiticar, S., Fieldhouse, B., 1995. A study of viscosity and interfacial tension of oils and emulsions.

Kim, C.K., Oh, J.H. & Kang, S.G., Information, C., 2016. A review of Deepwater Horizon Oil Budget Calculator for its Application to Korea. *J. Korean Soc. Mar. Environ. Energy*, 19(4), pp322-331, https://doi.org/http://dx.doi.org/10.7846/JKOSMEE.2016.19.4.322

Kinsman, B., 1965. Wind waves: their generation and propagation on the ocean surface.

Korea Institute of Ocean Science and Technology (KIOST), 2010. D/B establishment on characteristic of spilled oil and study on scientific use of dispersant.

Kujawinski, E.B., Kido Soule, M.C., Valentine, D.L., Boysen, A.K., Longnecker, K. & Redmond, M.C., 2011, Fate of dispersants associated with the Deepwater Horizon oil spill, *Environ. Sci. Technol.*, 45(4), pp.1298-1306.

Korea Maritime Institute (KMI), 2008. A study on advanced response system for oil spill.

Lee, M., Sung, H. & Kang, C., 2006. Development of guideline to use dispersants. J. Korean Soc. *Mar. Environ. Energy*, 9, pp.29-35.

Lee, Y.J.J. & Lee, Y.J.S., 2015. A Study on the Effectiveness and Safety Comparison of Dispersants. J. *Korean Soc. Saf.*, 30, pp.148-155.

Lehr, W., Jones, R., Evans, M., Simecek-Beatty, D. & Overstreet, R., 2002. Revisions of the ADIOS oil spill model. *Environ. Model. Softw.*, 17, pp.189-197. https://doi.org/10.1016/S1364-8152(01)00064-0

Lehr, W.J., 2001. Review of modeling procedures for oil spill weathering behavior. *Adv. Ecol. Sci.*, 9, pp.51-90.

Lessard, R.R. & DeMarco, G., 2000. The significance of oil spill dispersants. *Spill Sci. Technol.*, Bull. 6, pp.59-68. https://doi.org/10.1016/S1353-2561(99)00061-4

Lorenzo, T., Therrien, R. & Johannessen, B.O., 1995. Study of viscosity and emulsion effects on skimmer performance, in: *in Proceedings of 18th Arctic and Marine Oil Spill Technical Seminar*. Environment Canada, Ottawa, Canada.

Mackay, D. & Matsugu, R.S., 1973. Evaporation rate of liquid hydrocarbon spills of land and water. *Can. J. Chem. Eng.*, 51, pp.434-439.

Mackay, D. & Szeto, F., 1981. Effectiveness of oil spill dispersants - development of a laboratory method and results for selected commercial products. Inst. Environ. Stud. Univ. Toronto 63.

Mackay, D., Shiu, W.Y., Hossain, K., McCurdy, D. & Paterson, S., 1982. Development and calibration of an oil spill behavior model.

Monahan, E.C., 1971. Oceanic Whitecaps. *J. Phys. Oceanogr.*, https://doi.org/10.1175/1520-0485(1971)001<0139:OW>2.0.CO;2

Mooney, M., 1951. The viscosity of a concentrated suspension of spherical particles. *J. Colloid Sci.*, 6, pp.162-170. https://doi.org/10.1016/0095-8522(51)90036-0

Musk, S., 2011. Trends in Oil Spills from Tankers and ITOPF Non-tanker Attended Incidents.

Nordvik, A.B., 1995. The technology windows-of-opportunity for marine oil spill response as related to oil weathering and operations. *Spill Sci. Technol.*, Bull. 2, pp.17-46. https://doi.org/10.1016/1353-2561(95)00013-T

Payne, J.R., Kirstein, B.E., Mcnabb, G.D., Lambach, J.., Redding, R., Jordan, R.E., Hom, W., De Oliveira, C., Smith, G.S., Baxter, D.M. & Gaegel, R., 1984. Multivariate analysis of petroleum weathering in the marine environment - Sub Arctic. Volume I - Technical Results.

Reed, M., Johansen, Ø., Brandvik, P.J., Daling, P., Lewis, A., Fiocco, R., MacKay, D. & Prentki, R., 1999. Oil spill modeling towards the close of the 20th century: Overview of the state of the art. *Spill Sci. Technol. Bull.*, 5, pp.3-16. https://doi.org/10.1016/S1353-2561(98)00029-2

Renard, E.P., Clayton, J.R., Inlow, M., Hom, W. & Lee, S.E., 1995. Statistical evaluations of results of testing methods to evaluate performance of chemical dispersants for oil spills, in: Lane, P. (Ed.), The Use of Chemicals in Oil Spill Response, ASTM STP 1252. pp.55-91.

Rico-Mart?nez, R., Snell, T.W. & Shearer, T.L., 2013. Synergistic toxicity of Macondo crude oil and dispersant Corexit 9500A ® to the Brachionus plicatilis species complex (Rotifera). *Environ. Pollut.*, 173, pp.5-10. https://doi.org/10.1016/j.envpol.2012.09.024

Sebastião, P. & Guedes Soares, C., 1995. Modeling the fate of oil spills at sea. Spill *Sci. Technol. Bull.*, 2, pp.121-131. https://doi.org/10.1016/S1353-2561(96)00009-6

Song, B. & Springer, J., 1996. Determination of Interfacial Tension from the Profile of a Pedant Drop using Computer-Aided Image Processing: 1. Theoretical. *J. Colloid Interface Sci.*, 184, pp.64-76. https://doi.org/10.1006/jcis.1996.0597

Spaulding, M.L., 1988. A state-of-the-art review of oil spill trajectory and fate modeling. *Oil Chem. Pollut.*, 4, pp.39-55. https://doi.org/10.1016/S0269-8579(88)80009-1

Strøm-Kristiansen, T., Daling, P.S., Lewis, A. & Nordvik, A.B., 1993. Weathering properties and chemical dispersability of crude oils transported in US waters.

The International Tanker Owners Pollution Federation Limited, I., 2011. Use of Dispersants to Treat Oil Spills. Impact PR Des. Ltd. 4, 12.

United States Coast Guard (USCG), 1994. RRT VI IN-SITU BURN PLAN PART I (Operations Section). Eighth Coast Guard District, Hale Boggs Federal Building, 501 Magazine Street, New Orleans, Louisiana, 50.

Wise, J. & Wise, J.P., 2011. A review of the toxicity of chemical dispersants. *Rev. Environ. Health*, 26, pp.281-300. https://doi.org/10.1515/REVEH.2011.035

World Energy Conusil, 2016. World Energy Resources, World Energy Counsil. London EC3V 3NH, United Kingdom.

Zeinstra-Helfrich, M., Koops, W. & Murk, A.J., 2015. The NET effect of dispersants - A critical review of testing and modelling of surface oil dispersion. *Mar. Pollut. Bull.*, 100, pp.102-111. https://doi.org/10.1016/j.marpolbul.2015.09.022